AFRL-VS-HA-TR-98-0047

DEVELOPMENT OF METHODS TO GENERATE HIGH RESOLUTION CLIMATOLOGICAL DATABASES TO SUPPORT DOD MODELING AND SIMULATION PROGRAMS

John W. Zack
Glenn E. Van Knowe
Pamela E. Price
Mary D. Bousquet
Steve Young
Charles E. Graves

MESO, Inc.
185 Jordan Road
Troy, NY 12180

15 June 1998

Scientific Report No. 1

AIR FORCE RESEARCH LABORATORY
Space Vehicles Directorate
29 Randolph Road
AIR FORCE MATERIEL COMMAND
HANSCOM AFB, MA 01731-3010

"This technical report has been reviewed and is approved for publication"

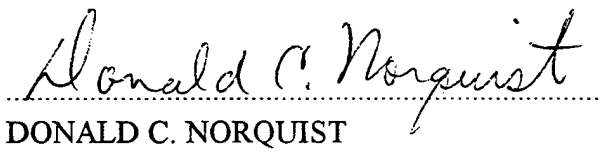

DONALD C. NORQUIST
Contract Manager

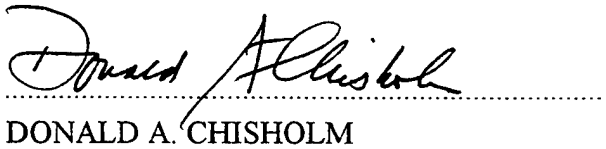

DONALD A. CHISHOLM
Branch Chief

This report has been reviewed by the ESC Public Affairs Office (PA) and is releasable to the National Technical Information Service (NTIS).

Qualified requestors may obtain additional copies from the Defense Technical Information Center (DTIC). All others should apply to the NTIS.

If your address has changed, if you wish to be removed from the mailing list, or if the addressee is no longer employed by your organization, please notify AFRL/VSOS-IM, 29 Randolph Road, Hanscom AFB MA 01731-3010. This will assist us in maintaining a current mailing list.

Do not return copies of this report unless contractual obligations or notices on a specific document require that it be returned.

REPORT DOCUMENTATION PAGE

Form Approved
OMB No. 0704-0188

1. AGENCY USE ONLY (Leave blank)	2. REPORT DATE	3. REPORT TYPE AND DATES COVERED
	15 June 1998	Scientific Report No. 1

4. TITLE AND SUBTITLE

Development of Methods to Generate High Resolution Climatological Databases to Support DOD Modeling and Simulation Programs.

5. FUNDING NUMBERS

F196828-97-C-0025

PR CLMS TAEA WUBA

6. AUTHOR(S)

John W. Zack
Mary D. Bousquet
Glenn E. Van Knowe
Steve Young
Pamela E. Price
Charles E. Graves

7. PERFORMING ORGANIZATION NAME(S) AND ADDRESS(ES)

MESO, Inc.
185 Jordan Road
Troy, NY 12180

8. PERFORMING ORGANIZATION REPORT NUMBER

10054-01

9. SPONSORING/MONITORING AGENCY NAME(S) AND ADDRESS(ES)

Air Force Research Laboratory
29 Randolph Road
Hanscom AFB, MA 01731-3010

Contract Manager: Donald Norquist / VSBE

10. SPONSORING/MONITORING AGENCY REPORT NUMBER

AFRL-VS-HA-TR-98-0047

11. SUPPLEMENTARY NOTES

None

12a. DISTRIBUTION/AVAILABILITY STATEMENT

Approved for public release; distribution unlimited

12b. DISTRIBUTION CODE

13. ABSTRACT *(Maximum 200 words)*

This project focuses on developing methods to estimate climate statistics at high resolution in data sparse and data rich locations. The method, given the name CLIMOD, is based on the use of a numerical-dynamical atmospheric model executed in data assimilation mode to generate a ten year sample of simulated data from which climatological statistics are computed. The major objectives of the project are to: (1) demonstrate the robustness and general applicability of the method; (2) refine the CLIMOD technique to optimally blend available observations and numerically simulated climate data; (3) extend the method to complex derived climate variables; and (4) construct an integrated software package that can be used anywhere in the world. The work during this first year included: (1) the development of a method to optimally blend the available observations and model generated data into a seamless regional climatology; (2) development of a method to objectively assess the quality of the simulated climate statistics in both data rich and data sparse regions; and (3) the generation of three-dimensional simulated climate statistics for all seasons of the year over a 10-year period for two different regions of the world: Korea and the Middle East.

14. SUBJECT TERMS

climate modeling, numerical modeling, numerical weather predication

15. NUMBER OF PAGES

16. PRICE CODE

17. SECURITY CLASSIFICATION OF REPORT	18. SECURITY CLASSIFICATION OF THIS PAGE	19. SECURITY CLASSIFICATION OF ABSTRACT	20. LIMITATION OF ABSTRACT
Unclassified	Unclassified	Unclassified	UL

TABLE OF CONTENTS

Foreword

The Defense Modeling and Simulations Organization (DMSO), through the Air Force Combat Climatology System Modeling and Simulation Division (AFCCC/MS) is supporting the Air Force Research Laboratory (Phillips Lab) contract F19628-97-C-0025. This contract is a three-year project to develop a method for estimating climate statistics at high spatial resolution in both data sparse and data rich regions. The method, given the name CLIMOD, is based on the use of a numerical-dynamical atmospheric model to generate a large sample of simulated atmospheric data from which climatological statistics are computed. The objectives of this project are to: (1) demonstrate the robustness and general applicability of the method by generating and evaluating climatological databases for all seasons in two climatologically distinct regions of the world that are of interest to DOD operations; (2) refine the CLIMOD technique to optimally blend available observations and numerically simulated data to produce the highest quality climate statistics; (3) Extend the technique to provide estimates of derived variables and additional statistical parameters that are frequently required by DOD applications; and (4) construct an integrated CLIMOD software package that can be efficiently used to generate high quality simulated climate statistics for any location in the world.

The work during the first year of the project includes: (1) development of a method to optimally blend the available observations and model-generated data into a regional statistical climatology; (2) development of a method to objectively assess the quality of the simulated climate statistics in data rich and data sparse regions; and (3) the generation of three-dimensional simulated climate statistics for all months of the year over a 10-year period for two different regions of the world: Korea and the Mideast.

The second year of the project will focus on: (1) the execution of data denial experiments to assess the impact of each data type on the quality of the climate statistics generated by the CLIMOD approach; (2) the development and implementation of methods to compute the statistics of derived variables from the basic meteorological variables produced by the model; (3) the use of the derived-variable computational procedures to generate climatological datasets for the derived variable for each of the two regions for which a climatology of basic variables was created in the first year; and (4) the development of methods to compute specialized statistics such as the probability of extreme events from the basic CLIMOD output.

The work during the third year will consist of: (1) the documentation and delivery of the derived variable climatological data to AFCCC; (2) the construction of an integrated CLIMOD software package which could be used to generate climatological databases or as a tool to further refine the CLIMOD technique; (3) delivery of the software package to AFCCC; and (4) the generation of three-dimensional simulated climate statistics for all months of the year over a 10-year period for a tropical region.

This interim report covers Tasks 1 through Tasks 4 of this project.

1.0 Introduction

There are multitudes of DoD simulation applications that require statistical values of various environmental parameters that describe the local 3-D climate in great detail. These applications include battle to global-scale simulations, real-world contingency ("what if") situations, and weapons system testing and development. The most obvious and direct way to obtain local climate statistics is to calculate them from long-term point observations. However, the use of long-term observational datasets imposes at least two limitations: (1) long-term point observational datasets are not currently available for many areas of the world; and (2) the representativeness and quality of observations change in time as observing sites are relocated, the land use around a site is changed or new instrumentation is used. An alternative is to generate statistics from a set of simulations using a limited-area high resolution mesoscale model that is based upon the physical processes of the atmosphere. This approach can be used to address two different types of applications. One type of application is to use the high resolution model to infer a set of climate statistics from a climatic state that has been generated by a General Circulation Model (GCM). The high resolution model is used to add additional detail to the GCM simulation. In this approach the high resolution model is essentially a nested model within the GCM. The initial and boundary condition data are extracted from the GCM output. Giorgi et al. (1993) used a version of the Penn State/NCAR mesoscale model to execute a 2-year simulation that used initial and lateral boundary data extracted from a GCM. This work was recently extended by Giorgi and Marinucci (1996).

In the second type of application, which is used in this project, the objective is to estimate the actual climate statistics for a particular period of time over a specified region. This is the objective that is most relevant to DOD simulation activities, because it can be used to simulate actual periods of records. This objective can be addressed by executing the model for a long period of time in a data assimilation mode and allowing the model to fuse the available data into a 3-D climatological dataset. In this mode the model continuously or periodically ingests the available observed data through one of several possible data assimilation techniques (Newtonian relaxation, periodic reanalysis, etc.). The model then dynamically fuses the available observations from the region of interest with its knowledge of the surface characteristics of the earth and the basic principles of physics to generate estimates of local climate statistics at all points on a three dimensional grid that covers the region. This technique has been given the name CLImate statistics by a dynamical MODel (CLIMOD). The climate results are likely to be much more representative of actual periods of record than results from the GCM-nested method. The CLIMOD technique is, in general, a more difficult approach than the GCM-nested application because the observed data must be inserted into the simulation in a way in which it will beneficially impact the resulting statistics. This is not a trivial problem because the data has quality and representativeness attributes that can sometimes cause it to conflict with the values generated by the model.

The Air Force Research Laboratory funded project , through the Air Force Office of Scientific Research (AFOSR), (AFOSR contract F4960-95-1-0523) has established a proof-of-

concept for the CLIMOD method. This project performed a set of experiments, which determined that the climate statistics produced by the CLIMOD technique are of very good quality if properly computed. However, the research also showed that the data assimilation strategies, PBL schemes, micro physics and the cumulus parameterization schemes employed in the model greatly influenced the quality of the statistics. This current research has demonstrated significant success in implementing new data assimilation strategies, PBL schemes and in selecting the appropriate micro physics and cumulus parameterizations for producing good quality climate statistics.

The numerical-dynamical model approach researched in this project has proven to have many advantages over the traditional interpolation approaches of generating climatological statistics from available observations including:

(1) the numerical-dynamical method has the capability of providing reasonable estimates of climate statistics in areas without any direct point observations;

(2) global-scale gridded analysis data exists for the past forty years to support applications of the method;

(3) a dynamically consistent 3-D climatology can be produced for any location on the earth;

(4) output can be used to calculate parameters for hydrology, aerosols and E-O weapon systems;

(5) it is a flexible tool which can be configured to provide information at virtually any required spatial and temporal scale;

(6) the method can be easily integrated with other databases to support the creation of "what if" scenarios; and

(7) it can be used to assess the impact of future changes in the environment such as urbanization, changes in land use and battlefield conditions on the climatological statistics.

The following personnel are involved in the research.

Name	TITLE/ORGANIZATION
Dr John Zack	Principal Investigator, MESO, Inc.
Dr Glenn Van Knowe	Sr. Research Scientist, MESO, Inc.
Dr Charles Graves	Lead Sub-Contractor, St. Louis University
Mr. Don Norquist	AFRL Contract Monitor, AFRL/VSBE
Capt. John Werner	Technical Monitor, AFCCC/SYT
Capt. Matt Doggett	Technical Monitor, AFCCC/CCX

2.0. DESCRIPTION OF THE CLIMOD APPROACH

The objective of the CLIMOD technique is to estimate the actual climate statistics for a particular period of time over a specified region. The approach used executes a numerical model for a long period of time in a data assimilation mode and allows the model to fuse the available data into a 3-D climatological dataset. A study done in conjunction with this research has shown that a recently developed form of data assimilation called Incremental Update Analysis (IAU) (Stauffer et al., 1991) produces the best results of the several data assimilation schemes evaluated. Through the IAU process combined with the model's knowledge of the surface characteristics of the earth and the basic principles of physics, the available observations of any specified region are dynamically fused to generate estimates of local (point) climate statistics at other locations in their region for which no observational climate data is available. Once the basic climate database is created, observed climatologies are used to improve the mean values and variability by compositing the observed data with the simulated data.

2.1 GENERAL SYSTEM DESIGN.

The CLIMOD method is designed to produce the simulated climatologies in a six step process. (1) The MASS model is used to simulate 10 years of hourly observations at a 10 and 40 km grid resolution. The simulations are generated in data assimilation mode with a nested grid system. A coarse grid with a 3-D grid point matrix size of 80x80 horizontal grid points on 20 vertical levels uses a 40 km horizontal grid spacing, while the fine mesh grid uses the same 3-D grid point matrix size but employs a horizontal grid increment of 10 km. Thus, the coarse mesh grid covers an area of approximately 3200 by 3200 km while the fine mesh operates on a theater scale area of approximately 800 by 800 km. Attachment 1 outlines the steps performed in the running of the model. (2) The model output is qualitatively checked through the runs for meteorological soundness. (3) Observational data is then blended with the simulated data to create a seamless database that maintains the best quality at every location. (4) Climate statistics are then generated for grids and specific locations within the fine mesh and coarse mesh domains. (5) Rigorous quantitative evaluation is made by comparing the composited climate statistics with observed climate data. This is done using a method developed for this project to establish the confidence the user can have in the data. (6) The data is then put into a standard format for storage.

The global grid point analysis dataset (e.g. the NCAR/NCEP GDAS Reanalysis dataset) and all available rawinsonde and surface data are being used to generate the climate grids. It is also theoretically possible to assimilate other types of data such as radiance data or derived sounding or cloud information from satellite sensors. The use of such data may have a significant beneficial impact on certain components (e.g. cloud climatology) of the climatological datasets. However, the use of such datasets is beyond the objectives and resources of this project. Nevertheless, this does represent an area in which future enhancements can be made to the CLIMOD method.

2.2 DATA DESCRIPTION.

a. Databases Defining the Surface Characteristics

Land Water Distribution. One of the most basic grid parameters that needs to be determined is whether a grid box is composed of land or water. An integer indicator or flag is used to determine land or water where "0" indicates water and "1" indicates land. The database used to determine the land/water flag is a U.S. Navy dataset obtained from the National Center for Atmospheric Research (NCAR). The resolution of the dataset is approximately 18 km in the mid-latitudes.

Terrain Elevation. The database used to describe the terrain elevation for each model grid box is the U.S. Central Intelligence Agency 5 minute global terrain dataset. The resolution of this data base is approximately 9 km.

Sea Surface Temperature (SST). The MASS uses SST data from global sea surface temperature climatological datasets. One dataset is used for each month of the year at a 1 degree latitude-longitude resolution.

Land use and Land cover. The MASS land use/land cover dataset is based on the Anderson Level II classification scheme (Anderson et. al., 1976) developed by the U.S. Geological Survey (USGS). The Anderson Level II land use scheme provides 10 basic land use choices, such as urban, agricultural, range, wetland, etc. and further divides each major category to give a total of approximately 50 choices. The resolution of the land use/land cover is 5 x 5 degree latitude-longitude sectors.

Soil-type Classification. A soil classification database is also used in the MASS.

Normalized Difference Vegetation Index (NVDI). Data providing information on the vegetation is also used in the MASS. The basic data has been collected by the Advanced Very High-Resolution Radiometer (AVHRR) instrument. The NVDI used is derived by calculating the normalized difference between two AVHRR channels, the near infrared and the visible. The resolution of NDVI dataset is 5 x 5 degree latitude-longitude sectors.

b. Atmospheric Databases

Research was done on the potential of using the NCEP/NCAR 40 Year Reanalysis Project datasets from NCAR as an improved source of data to initialize and provide lateral boundary conditions. The Reanalysis Project data is available every six hours versus every 12 hours for Global Optimum Interpolation (GOI) data datasets used in the proof-of-concept grant. MESO had to first develop a reader that converts the Reanalysis Project data format into a MASS readable format. MESO then performed tests on the Reanalysis Project data comparing its quality with the previously used Global Optimum Interpolation datasets. It was found that using the Reanalysis data better limits climate drift of the model and is an improvement over the

GOI datasets. The specific dataset used in the project is: ds090.0 1 January 1973 to 31 Dec 1982 from NCEP/NCAR Reanalysis Archive.

The 10 years of rawinsonde data were also obtained from the NCAR dataset: ds353.4 RAOBS and PIBALS Global Data for 01 Jan 1973 - 31 Dec 1982.

The surface data used was obtained from the Air Force Combat Climatology Center (AFCCC) DATSAV data. A reader was constructed to convert the DATSAV into a format readable by MASS.

2.3 DESCRIPTION OF THE MESOSCALE MODEL

The simulation model used in this project is version 5.11.2 of the Mesoscale Atmospheric Simulation System (MASS) model (Kaplan et al. 1982; MESO, 1995; Manobianco et al., 1996). The MASS is a three-dimensional primitive equation hydrostatic numerical model.

a. Basic Model Equations and Grid System

The basic model formulation, equations and grid system are fully described in the *MASS Version 5.6 Reference Manual* (MESO, Inc., 1994). The MASS uses the σ_p vertical coordinate described as

$$\sigma_p = \frac{p - p_t}{p_s - p_t}, \qquad (2.1)$$

where p is the pressure at the level, p_s represents pressure at the surface and p_t represents pressure at top of model domain. The MASS can be run using either a polar stereographic or mercator map projection. For this experiment the polar stereographic projection was used employing the map scale factor $m = 1 + \sin(\phi)/1 + \sin(\phi_0)$, where ϕ denotes any latitude and ϕ_0 denotes the reference latitude. The MASS uses an unstaggered horizontal grid and a staggered vertical grid. The atmospheric portion of the MASS consists of a hydrostatic system of seven model prognostic variables: u-wind component, v- wind component, pressure, temperature, humidity as water vapor mixing ratio, precipitation moisture, and cloud moisture.

Horizontal finite differencing is done using a fourth order scheme. Time marching is accomplished by using the split explicit scheme. A forward backwards scheme is used for the capture of inertial gravity waves. Advection is handled using the Adams-Bashford scheme (Meisinger and Arakawa, 1976).

The MASS surface energy budget is formulated after Noilhan and Planton (1989), which is based on the original work of Blackadar (1976, 1979). The MASS calculates the major impacts of both short and longwave radiative transfer on heating the ground surface, clouds and atmosphere. There are three radiative situations (clear, cloudy ,and partly cloudy) considered in the MASS for

long and shortwave radiation. The fractional sky cover is estimated based on a relative humidity-cloud fraction relationship at each model level. Walcek (1994) calculated the observed cloud cover-relative humidity relationships for an early spring midlatitude cyclone over land. The main observed difference is the approximate 20% increased cloud cover with relative humidities between 20-80%.

The solar radiation wavelengths, referred to as shortwave radiation, considered in the MASS ranges from 0.3-4 micrometers. The solar radiation is further divided into a visible (0.3-0.75 micrometer) and an infrared (0.75-4.0) micrometer band. The terrestrial or longwave radiation ranges from 4.0 to 50 micrometers and accounts for longwave radiative transfer from both the ground and the clouds.

For shortwave absorption in clear skies the direct radiative heating of the atmosphere (shortwave radiative flux divergence) is ignored. Only the radiative heating due to the shortwave irradiance received at the ground is parameterized. Rayleigh scattering and Mie scattering is accounted for at the molecular and particulate size level as the shortwave radiation passes through the atmosphere. The impact on the zenith angle due to terrain slope is also taken into account. The basic relationship, integrated at each model level, used to calculate shortwave radiation reaching the ground during clear sky conditions is $R_s\downarrow(k) = (1 + \Delta t - \Delta a)R_s\downarrow(k+1)$; where $R_s\downarrow(k)$ denotes radiation reaching level k from the level above and k+1 Δt represents the change in transmissivity from k to k+1; Δa defines the change in absorptivity from k to k+1. For cloudy sky conditions, the shortwave radiation is partitioned into the visible and infrared bands. The total solar radiation reaching the ground during cloudy conditions is calculated by $R_s\downarrow(\text{cloudy}) = t_{vis}R_{so}\downarrow(\text{vis}) + t_{ir}R_{so}\downarrow(\text{ir})$, where t_{vis} is the transmissivity in the visual range of the radiation spectrum, $R_{so}\downarrow(\text{vis})$ represent the solar constant at the top of the atmosphere in the visual spectrum, t_{ir} represent the transmivvity in the infrared spectrum, and $R_{so}\downarrow(\text{ir})$ represent the solar constant at the top of the atmosphere in the infrared part of the spectrum,. For partly cloudy conditions, the clear and cloudy downward shortwave irradiances are weighted by the total column cloud fraction as follows:

$R_s\downarrow(\text{partly cloudy}) = (1\text{-frac}_{col})\, R_{so}\downarrow(\text{clear}) + \text{frac}_{col}R_{so}\downarrow(\text{cloudy})$,

where R_{so} is the solar constant, frac_{col} equals cloud fraction for the entire column.

The parameterization of longwave radiative transfer, used to account for longwave cooling and heating of the ground and atmosphere, uses the broadband approach of Sasamori (1972) as described by Pielke (1984). The effects of water vapor and carbon dioxide longwave radiation absorption are parameterized. In the cloudy sky conditions the effective emissivity of the cloud is also taken into account. In the partly cloudy situation, the clear and cloudy longwave fluxes are combined. The longwave radiative process is partitioned into downward $\Delta R_L\downarrow$ and upward $\Delta R_L\uparrow$fluxes for the clear and cloudy cases.

b. MASS Planetary Boundary Layer

Two options exist for the MASS model planetary boundary layer formulation. The first closely follows the high resolution PBL model described by Zhang and Anthes (1982), which is

mostly based on the work of Blackadar (1976, 1979). This scheme has been used for many years by several modeling groups with good results. Some of the changes in the scheme from the original Zhang and Anthes paper are derived from changes made in the MM4 version of the Penn State/NCAR mesoscale model (Stauffer, 1992). A vertical profile of temperature, water vapor mixing ratio, and u- and v-components of wind on an arbitrary set of pressure levels are passed into the scheme, along with relevant surface characteristics. The result of the scheme is the calculation of time tendencies of each of the four variables listed above, along with some diagnostic PBL parameters, such as the depth of the boundary layer.

The second option is based on the work of Therry and LaCarrere (1983). It is a so-called 1.5 order closure scheme in which there is a prognostic equation for turbulent kinetic energy (TKE) and the turbulent mixing coeffiecient is a function of TKE. The boundary conditions were taken from Mailhot and Benoit (1982).

The MASS model divides the Planetary Boundary Layer (PBL) into two layers. The lower layer represents the surface or constant flux layer, the upper or above surface layer represents the Ekman layer. The Blackadar and TKE schemes are virtually identical in the surface layer. The differences are in the above surface layer. The MASS surface layer formulation is founded on separating the PBL into four regimes based on stability to calculate the scaling parameters. The criteria used to choose among three stable regimes and one unstable regime is the ratio of the PBL height (h) and the Monin-Obukhov length (L) combined with the bulk Richardson number (Rb).

The critical value of h/L = 1.5 is used to separate unstable (free convective) from three stable regimes. If h/L is equal to or less than 1.5 than Rb is used to identify which stable regime is used. The totally stable regime occurs when Rb is greater than 0.2. The damped mechanical turbulence regime is used when Rb is between 0 and 0.2. When Rb is equal to or less than zero, a forced convective regime is invoked. Each regime has different values of heat, moisture and momentum coefficients as described in the MASS Reference Manual (1995).

The MASS model's three stable and one unstable (convective) surface PBL regimes are calculated using the following method. First, profiles of four variables are used as input: temperature, moisture (mixing ratio), u wind component and the v wind component. The criteria for

$$R_b = (g \quad Z_a/\theta_a)(\theta_a - \theta_g)/(V_a)^2, \tag{2.2}$$

selection of a regime is based on Rb and h/L, Specifically,

where: Z_a equals height of first model level
g is acceleration of gravity
θ_a equals potential temperature at the first model level
θ_g equals potential temperature at the equals ground surface and
V_a equals wind velocity at the first model level.

For the three stable regimes the scaling parameters for heat, moisture and momentum are set

to be equal. That is $\psi_h = \psi_q = \psi_m$, where *h* denotes heat, *q* denotes moisture, and *m* denotes momentum. In the MASS only ψ_h and ψ_m are used. The Rb criteria distinguishes which stable layer is used. Two stable basic types of stable layers are possible. If Rb > 0, stability is indicated with little wind shear. If Rb > 0.2, the most stable regime results, with only weak turbulence allowed. For the most stable regime, the frictional velocity u* = 0.1 (land) and 0.0 (water) and the scaling parameter $\psi = -10 \ln(z_a/z_0)$. If 0 > Rb < 0.2 (between 0 and 0.2), then the damped mechanical turbulent regime results where the scaling parameter $\psi = -5(Rb/(1.10-5Rb)\ln(z_a/z_0)$.

If Rb < 0, you must go to h/L to determine if it is a stable (forced convective) or unstable (free convective) regime. If h/L is less than 1.5, forced convection results. With forced convection, the scaling parameters are set equal to 0 and the boundary layer depth is set to the first level above the surface layer where $\theta \geq \theta_a$. If h/L is greater than 1.5, unstable free convection results with the scaling parameters not set to be equal.

The stable regime tendencies are calculated from the following basic relationship:

$$\frac{\partial \chi}{\partial t} = \frac{(\chi_g - K_m \chi_1)}{\rho \Delta z_1}, \tag{2.3}$$

where χ, represents any variable, χ_g is the value of the variable at the surface, χ_1 is the value at the first model level, K_m is the eddy viscosity defined in "K-Theory" (Stull, 1988), ρ is the density, and $\Delta z1$ is the depth of the first model level. Heat flux at the top of the layer is calculated from a linear approach.

For the unstable free convective regime the tendency equations are based on the principle that a fraction of the total mass is being transferred between the surface layer and each PBL layer. The fraction of mass (m) exchanged between any level and the surface layer per unit time is as follows:

$$\overline{m} = \frac{H_1}{\rho c_p (1 - E_m) \int_{z_1}^{z_m} (\theta_a - \theta(z)) dz}, \tag{2.4}$$

where E_m is an entrainment parameter set to 0.2 and z_m is the height of the level where a rising parcel of air loses its buoyancy. The heat flux is calculated using a non-linear term.

The Blackadar and TKE scheme have significantly different formulations in the above surface or Ekman layer. The Blackadar sceme uses the K-theory approach as described by Blackadar (1976). All of the stable layers use the K-theory approach in the Ekman layer where $K_m = K_h = K_q$ is assumed which relates the turbulent flux to the associated mean variables. In the MASS the vertical diffusivity coefficient terms K_h and *Km* are calculated from use of the second

order shear term and the local Richardson number. Specifically, K_m is calculated from

$$K_m = \begin{cases} K_{z0} + S^{1/2}(kl)^2 \dfrac{Ri_c - Ri}{Ri_c}, if\ Ri < Ri_c \\ K_z 0, if\ Ri \geq Ri_c . \end{cases} \quad (2.5)$$

Where Ri is the local Richardson number, Ri_c is the critical Richardson number, K_{z0} is the background diffusivity, S is the vertical wind shear, l is the mixing length set to 100 m., k is the von Karman constant. The value of K is obtained from the K-Theory relationship which is $u'X = -K \partial X/\partial z$ where X denotes any of the variables.

For the free convective regime the local exchange coefficient is used above the mixed layer. Within the mixed layer the tendency equations are based on the fractional mass (m) exchanged between layers described in

$$\partial X/\partial t = \overline{m}(X_a - X), \quad (2.6)$$

where X represents any of the model variables.

TKE scheme calculates the tendencies above the surface layer using the prognostic equations for the 1.5 order closure scheme as outlined by Stull, (1988).

$$\frac{\partial \bar{U}}{\partial t} + \bar{U}\frac{\partial \bar{U}}{\partial x_j} = f_c(\bar{V} - \bar{V}_g) - \frac{\partial(\overline{u'w'})}{\partial z} \quad (2.7)$$

$$\frac{\partial \bar{V}}{\partial t} + \bar{U}\frac{\partial \bar{V}}{\partial x_j} = -f_c(\bar{U} - \bar{U}_g) - \frac{\partial(\overline{v'w'})}{\partial z} \quad (2.8)$$

$$\frac{\partial \bar{\theta}}{\partial t} + \bar{U}\frac{\partial \bar{\theta}}{\partial x_j} = \frac{1}{\bar{\rho}C_p}\frac{\partial Q_j^*}{\partial x_j} - \frac{L_v E}{\bar{\rho}C_p} - \frac{\partial(\overline{\theta'w'})}{\partial z} \quad (2.9)$$

$$\frac{\partial \bar{C}}{\partial t} + \bar{U}\frac{\partial \bar{C}}{\partial x_j} = \frac{S_c}{\rho_{air}} - \frac{\partial(\overline{c'w'})}{\partial z} \quad (2.10)$$

$$\frac{\partial \bar{e}}{\partial t} + \bar{U}\frac{\partial \bar{e}}{\partial x_j} = \frac{g}{\theta_v}\left(\overline{w'\theta_v'}\right) - \overline{u_i'w'}\frac{\partial \bar{U}_i}{\partial z} - \frac{\partial\left[\overline{w'\left((p'/\rho) + e\right)}\right]}{\partial z} - \varepsilon \qquad (2.11)$$

The general notation is as follows:

1. Mean quantities are generally capitalized with an overbar ($\bar{\cdot}$). They are the west-to-east, south-to-north and vertical components of velocity ($\bar{U}$, $\bar{V}$, $\bar{W}$), potential temperature $\bar{\theta}$, pressure $\bar{P}$, tracer/moisture variable mixing ratio $\bar{c}$, density $\bar{\rho}$ and turbulent kinetic energy e.
2. Perturbations from the mean for a given volume for the above variables are denoted by a prime ('), for example, u';
3. The value of the perturbation quantities derived through a Reynolds averaging procedure have an overbar, for example $\overline{u'}$ or $\overline{u'w}$;
4. Some terms use a subscript j to represent all three cartesian directions. For example, U_j refers to the three wind components and x_j refers to the three directions. Consequently, $\bar{U}\frac{\partial \bar{U}}{\partial x_j}$ is shorthand for $\bar{U}\frac{\partial \bar{U}}{\partial x} + \bar{V}\frac{\partial \bar{U}}{\partial y} + \bar{W}\frac{\partial \bar{U}}{\partial z}$.

The terms on the left hand side in each equation represent the local tendency and advection, respectively. Equations (2.7) and (2.8) describe the evolution of the two horizontal components of momentum. The first term on the right hand side represents the effects of the Coriolis and pressure gradient forces. The last term represents turbulent fluxes. Equation (2.9) describes the evolution of the potential temperature. The terms on the right hand side represent the contributions of radiation, water phase changes and turbulent fluxes, respectively. Equation (2.10) describes the evolution of a particular phase of water (vapor, solid, liquid) or some other passive tracer C. The first term on the right hand side represents sources or sinks (condensation, evaporation, etc) while the second represents turbulent fluxes. Equation (2.11) is the TKE budget equation. The terms on the right hand side represent buoyant production/loss, mechanical or shear production/loss, turbulent transport and redistribution by pressure perturbations, and viscous dissipation, respectively.

The general expression for the parameterization of the second order fluxes and other terms are:

$$\overline{u'w'} = -K_m\frac{\partial \bar{U}}{\partial z} \qquad (2.12)$$

$$\overline{v'w'} = -K_m\frac{\partial \bar{V}}{\partial z} \qquad (2.13)$$

$$\overline{c'w'} = -K_H\frac{\partial \bar{C}}{\partial z} \qquad (2.14)$$

$$\overline{w'\theta'} = -K_H \frac{\partial \bar{\theta}}{\partial z} - \gamma_c \qquad (2.15)$$

The second term on the right hand side of (10-97) allows for counter gradient buoyancy fluxes under unstable conditions.

The eddy diffusivity coefficients and dissipation of TKE are:

$$K_m = 0.5 l_k \bar{e}^{1/2} \qquad K_H = 1.35 K_m \qquad (2.16)$$

and

$$\varepsilon = \frac{\bar{e}^{3/2}}{8\, l_\varepsilon} \qquad (2.17)$$

l_k and l_ε l_k and l_ε Therry and Lacarrere (1983) who used the results of a third order closure simulation to parameterize them as variables rather than constants. They parameterize l_k and l_ε as as rather complicated functions of the PBL depth, the local height above ground level, the local stability:

$$l_\varepsilon = \frac{1}{\frac{1}{kz} + \frac{15}{h} - \left(\frac{1}{kz} + \frac{5}{h}\right) m_1 m_2 + \frac{1.5}{l_s}} \qquad (2.18)$$

$$m_1 = \frac{1}{1 + 0.005 \frac{h}{kz}} \qquad m_2 = \begin{cases} \dfrac{1}{1 - \frac{l_{mo}}{h}} & l_{mo} < 0 \\ 0 & l_{mo} \geq 0 \end{cases} \qquad (2.19a \text{ and } b)$$

$$l_s = \left(\frac{\bar{e}}{\beta \frac{\partial \bar{\theta}}{\partial z}}\right)^{0.5} \qquad h = \begin{cases} h_{pbl} & \text{surface layer heat flux is upward} \\ \dfrac{0.3 u_*}{f} & \text{surface layer heat flux is downward} \end{cases} \qquad (2.20a \text{ and } b)$$

$$l_k = \frac{1}{\frac{1}{kz} + \frac{15}{h} - \left(\frac{1}{kz} + \frac{11}{h}\right) m_1' m_2' + \frac{3}{l_s}} \qquad (2.21)$$

$$m_1' = \frac{1}{1 + 0.0025 \frac{h}{kz}} \qquad m_2' = m_2 \qquad (2.22a \text{ and } b)$$

where z is the height above the ground and k is von Karman's constant (0.4). The countergradient term in the vertical temperature flux term, γ_c, is parameterized as:

$$\gamma_c = \frac{5g\theta_*^2}{\theta w_*^2} \tag{2.23}$$

where $\theta_* = \frac{\overline{w'\theta'}_s}{w_?}$ and $w_* = \left[\frac{g\overline{w'\theta'}_s z}{\bar{\theta}}\right]^{1/3}$. The subscript s refers to the surface layer while z refers to height above ground level. Finally, the fourth term in the TKE budget equation, is parameterized as:

$$\frac{\partial}{\partial z}\left[\overline{w'e} + \overline{p'w'}/\rho_0\right] = 0.5\frac{\partial}{\partial z}\left[l_k \bar{e}^{1/2}\frac{\partial \bar{e}}{\partial z} - \frac{0.5 l_\varepsilon \bar{e}^{-1/2} g w_* \overline{w'\theta'}}{\theta}\right] \tag{2.24}$$

In the lowest model layer which is considered to be the surface layer, the TKE is set to:

$$e_s = \begin{cases} 3.75u_*^2 & \text{(stable)} \\ 3.75u_*^2 + 0.2w_*^2 + \left(\frac{-z_s}{L}\right)^{2/3} u_*^2 & \text{(unstable)} \end{cases} \tag{2.25}$$

The atmosphere is considered to be unstable if potential temperature decreases with height between the surface and the lowest model layer above the surface.

c. MASS Soil Hydrology

The soil hydrology scheme is based on Mahrt and Pan (1984) model. The soil is divided into a shallow 5 cm deep surface layer and a deeper 5-30 cm layer. The plant roots are assumed to be in the deeper layer. A surface "cover" moisture reservoir is parameterized to account for intercepted rainfall. The hydrology scheme uses the land use, soil type and vegetation index data for its computations.

The soil moisture budget takes into account the precipitation that falls, the amount that is intercepted by the surface, and the amount that infiltrates into the soil. The model also accounts for the diffusion of moisture in the soil, and the evaporation of bare soil and vegetation.

The effects of snow cover are also parameterized in the model. The albedo (which is by far the most important), evaporation rates, and roughness length are all altered to account for snow cover.

d. MASS Moisture Physics

The MASS handles the moisture physics and latent heating on two scales. The larger scale

is handled as grid-scale processes explicitly calculating the latent heating at each grid point. The convective latent heating is handled through sub-grid scale parameterization.

The grid scale moisture physics can be handled in two ways. One method employs a diagnostic scheme precipitating all liquid and frozen water out of the atmosphere. This is the scheme employed in the 40 km horizontal courser mesh nest. The other option is a prognostic scheme, which accounts for the phase change processes involving both the cloud size, water droplets, and ice crystals as well as the precipitation size raindrops and snow. The major disadvantage of using the prognostic scheme is the increased computational time. The prognostic scheme is used in the 10 km horizontal finer mesh nest.

Convective latent heating is handled through the use the of Kuo-Anthes (Kuo 1965; Anthes 1977) parameterization scheme. The Kuo-Anthes scheme uses the principle that the magnitude of the convective scale heating is proportional to the grid scale moisture supply.

2.4 MASS Configuration for CLIMOD.

Several issues concerning the quality of the data, model run time and model configuration were determined through evaluating the results of the proof-of-concept project as they pertain to the current research. The primary issues investigated and resolved are: (1) which planetary boundary layer scheme to use, (2) which cumulus scheme to use, (3) moisture physics issues (4) and how to solve problems during periods of data assimilation. Much of the early testing focused on determining the "best" model configuration for the climate runs. Utilizing the test results, modifications were made to the model making it more optimal for climate purposes.

Because the focus of the climate project is to improve the capability of simulating climatologies near the earth's surface, a comparison was made using the two MASS PBL schemes: the traditional Blackadar scheme and the TKE PBL scheme based on turbulent kinetic energy. The comparison used the results from the proof-of-concept research as well as results from additional investigation of the subject as part of this project. The comparison determined that TKE produced superior results for the temperature, dew points and wind speeds.

It was observed that a small but significant drying of the simulated atmosphere occurred each time rawinsonde data was assimilated into a model run through the Newtonian Relaxation or 'nudging" scheme based upon an algorithm that is similar to that used by Stauffer et al. (1991). This resulted in a strong low-cloudiness and precipitation bias for the first three hours of the simulation (0-3 UTC). The reason for this was determined to be the slight low humidity bias in the rawinsonde data combined with the nudging method over-forcing the model solution to the dry biased observed rawinsonde data. The specific details of the simulation strategy that is being employed to generate the 40 km and 10 km databases were determined from the results of the analysis of simulation experiments that were completed in the proof-of-concept. The issues investigated were (1) the types of data that will be assimilated into the simulations; (2) the frequency of the data assimilation; and (3) the method used to assimilate the data.

The first major issue of data assimilation addressed was what type of data to use. The global grid point analysis dataset (e.g. the NCAR/NCEP GDAS Reanalysis dataset) was determined to be the best available choice for initialization and lateral boundary conditions. The next task was to determine which was the best strategy of using the available rawinsonde and surface data. There were some issues concerning the impact of data assimilation within the planetary boundary layer. For example, based on their experiments with the PSU/NCAR model, Stauffer et al. (1991) recommend that surface temperature data not be used in a Newtonian relaxation data assimilation scheme within the planetary boundary layer. They note that the continuous assimilation of surface temperature data can have a negative impact on the model's boundary layer parameterization scheme. Analysis of the experiments performed in the proof-of-concept project suggested that the assimilation of surface data can, at times, have a negative impact on the near-surface component of the model simulation. However, even with the problems of assimilating observed data, it was found that the addition of observed surface and rawinsonde data helps remove the model drift. It was further determined that it is theoretically possible to assimilate other types of data such as radiance data, derived soundings, or cloud information from satellite sensors. The use of such data may have a significant beneficial impact on certain components (e.g. cloud climatology) of the climatological datasets. However, the use of such datasets is beyond the objectives and resources of this project. Nevertheless, this does represent an area in which future enhancements can be made to the CLIMOD method.

The second major issue addressed was the frequency of data assimilation. An intuitive approach would be to assimilate the data at the same frequency at which it is observed. In this approach, rawinsonde data would be assimilated at 12-hour intervals and surface data would be assimilated at hourly intervals in regions where it is available at that frequency, and at 3 hour or 6 hour intervals, in other areas. However, it was found that frequent data assimilation can have some drawbacks due to characteristic problems with certain types of data. For example, rawinsonde data tends to have a dry bias in atmospheric environments that are near saturation. Thus, the assimilation of rawinsonde moisture data can have the effect of erroneously reducing the amount of cloud cover and precipitation produced in a model simulation. Therefore, the assimilation of rawinsonde moisture data at more frequent intervals can generate more of a dry bias in a simulation. This is less of a problem in forecast simulations because the model will spin-up to the proper degree of saturation in a few hours after initialization and then be unencumbered by the rawinsonde dry bias. However, in a simulation to generate climatological datasets, the repeated assimilation of rawinsonde data can, for example, introduce a dry bias into the cloud and precipitation climatologies

In an attempt to maximize the positive aspects of using observed data to remove model drift and to minimize the negative impact of observed biases, it was determined that the impact of different data assimilation strategies on the resulting climatological databases needed to be investigated further as part of this project. The results of the data assimilation experiments were used as a guide for selecting the strategy to be used for the generation of the climatological databases for Korea and the Middle East.

There were many possible candidates for the four-dimensional data assimilation method. However, some are too computationally intensive (e.g. the adjoint technique) or, as yet,

unproven to be used in this project. The two methods that have been widely used and are computationally manageable are: (1) discontinuous data assimilation through periodic objective analyses using the simulation output as a first-guess; and (2) continuous data assimilation through the use of Newtonian relaxation (also known as "nudging"). The discontinuous approach has been widely used in operational forecast centers to initialize forecast simulations. For example, the 12-hour forecast from a previous run is used as a first-guess for the initialization analysis for the next forecast simulation. The advantage of this approach is that model simulation is interrupted only at specific times and the model physics control the simulation between those times. Thus, the model physics can overcome biases in the data that are not consistent with the model physics. This can be an asset or a liability depending on the quality of the model physics and the data.

In the Newtonian relaxation approach, additional terms are added to the model equations to assimilate the data. The model simulation is then continually nudged towards the data. This approach minimizes the shock to the model that is often generated by the reanalysis procedure in the discontinuous data assimilation approach, and also permits data from any time period to be easily used in the data assimilation process. However, there are problems with the Newtonian relaxation approach. The presence of an additional non-physical term in the model equations means that the result of the simulation does not satisfy the true model equations unless the data assimilation term is zero (i.e. the model value and the observed value of a variable are identical at a point). This would not be a significant issue if all the data had no errors and were representative of the model grid scale. Of course, that is not the case. Therefore, continuous data assimilation can introduce biases into the model simulations. An example is the previously cited problems with rawinsonde moisture data. Continuous assimilation of rawinsonde moisture data can introduce a dry bias into a simulation. Some modelers have addressed this problem by using a lower nudging coefficient for the assimilation of rawinsonde moisture data (e.g. Stauffer et al., 1991). Of course, this also reduces the impact of the moisture data on the entire simulation.

Thus, it is not intuitively obvious which method would yield the best climatological statistics. It is even possible that one method may produce better results for some variables while another method will yield better results for other variables. Experiments with both of these techniques were executed as part of the current project. These results provided guidance for the selection of the method to be used for the simulations over Korea and the Middle East.

The simulation strategy which was used in the proof-of-concept experiments is schematically illustrated in Attachment 2. This strategy represents one of the options that could of been employed in the current project. In this approach, a coarse mesh simulation (40 km grid) was initialized at 0000 UTC on the first day of each month for each region. This simulation is initialized from an optimal interpolation (OI) analysis which uses a first guess field from a large scale gridded analysis and all available rawinsonde and surface data. The large-scale data used in the proof of concept was the NCEP GOI data. The GDAS Renalysis data is being used in the current project. The coarse mesh model was then executed for 24 hours using the large scale interpolated gridded analysis data (NCEP GOI data) at 12-hour intervals to specify the lateral boundary conditions. The current project is using GDAS Renalysis data every 6 hours. The data from the 24th hour of this simulation was then used as the first guess for the initialization

analysis of the next simulation. Once again, rawinsonde and surface data were used to update the first guess. In this scheme, the fine mesh (10 km grid) simulation was initialized at 0000 UTC on the first day of each month by interpolating the initialization dataset of the coarse mesh grid. The fine mesh model is then executed for 12 hours. The lateral boundary condition data was taken from the hourly output of the 40 km simulation. The data from the 24th hour of the 10 km simulation was used to serve as the first guess for the initialization of the subsequent fine mesh simulation. All available rawinsonde and surface data are used to update the first guess. All of the fields describing the state of the earth's surface (soil moisture, snow depth etc.) were carried through the reinitialization process. Thus, the subsequent simulation begins with the values existing at the end of the previous simulation. If data such as observed snow cover were available, then it probably would have been beneficial to assimilate it into the simulations. Unfortunately these types of data are not typically available in many parts of the world.

The data assimilation scheme ultimately selected for the current project was Incremental Update Analysis (IAU). MASS was used to assess the IAU scheme. The implementation of IAU in MASS required: (1) the modification of the data preprocessor so that it can write analysis increments rather than actual grid point values when preparing for an IAU; and (2) modifying the model so that it can read the IAU file written by the preprocessor, transform it to a time tendency and add this tendency to the model variables at each grid point during the IAU period. A 31-day series of MASS simulations extending from 1 January to 31 January 1990 was selected to compare the performance of the IAU, Newtonian relaxation and intermittent data assimilation (optimal interpolation) schemes. This time period was chosen because MESO had already been performed intermittent assimilation and Newtonian relaxation experiments for this period. A schematic of the simulation strategy used in this IAU experiment is shown in Attachment 3. After the first 12 hour simulation (simulation A), each subsequent simulation was run for 18 hours. The first 6 hours of each 18 hour simulation overlapped with the previous simulation so that an IAU could be performed during this period. The 6-hour interval was considered to be the assimilation period which produced an initialization dataset valid at the end of the interval. The last 12 hours of each 18 hour simulation (e.g. simulation B) was evaluated as a forecast. In this approach, each day consisted of two 12-hour forecasts. Each of these forecasts is initialized with an IAU data assimilation procedure with the exception of the first simulation on the first day (simulation A) which is initialized with an optimum interpolation analysis of rawinsonde data employing an NCEP GOI as a first guess. The net result was a significant reduction of the biases in the moisture related variables relative to the other data assimilation schemes while retaining the observational control of model drift.

Attachment 4 shows all the data assimilation schemes considered for this project. It was determined that it is best to use a 12 hour data assimilation of all available surface and rawinsonde data to control model drift. To reduce the influences of the biases in the observed data IAU was implemented as the data assimilation scheme. IAU is employed during the first three hours after the assimilation of observed data. First IAU to calculates model and observed data tendencies. The tendencies are then used to gently push the simulation to the observed solution without forcing the observed biases into the model. The result has been a significant

improvement in the moisture-related variables relative to the other data assimilation schemes during the first few hours of the simulations.

Another significant factor is the microphysics employed. Our evaluation showed that to optimize results, we needed to use a complex prognostic microphysical package which incorporates phase changes of the moisture in the atmospheric. Using simple traditional diagnostic microphysical routines significantly degraded the moisture related climate statistics. Unfortunately, the more optimal climate run configurations are also more computationally intensive. It was jointly decided that the better results justified the increase in run time.

The final model configuration selected was:

(a) Data assimilation: Assimilate all available rawinsonde and surface data using IAU every 12 hours using a 3 hr assimilation period

(b) Model physics for the coarse mesh (40 km): The Blackadar planetary boundary layer scheme, a modified version the Kou- Anthes cumulus scheme and diagnostic moisture physics were all chosen for computational efficiency.

(c) Model physics for the fine mesh (10 km): The TKE planetary boundary layer scheme; the Fritsch-Chappell cumulus scheme and prognostic moisture mixed phase explicit physics with prediction variables for cloud ice, cloud water, rain water and snow layer were all chosen to optimize the results at the higher resolution.

It would be optimal to use the TKE boundary scheme for both runs. However, TKE takes longer although it is somewhat better for producing accurate low-level fields. The choice of Blackadar is intended to speed up the production process. The choice of Blackadar has less of an impact on the 40 km results than on the 10 km results. Fritsch-Chappell handles the small-scale convective precipitation better than the Kuo-Anthes at the 10 KM resolution. The explicit physics scheme is more computationally expensive but it does produce superior results, especially at the higher resolution of 10 Km.

An example of the geographical domains for the coarse (40 km) and fine (10 km) grids for each region is presented in Attachments 5 and 6.

2.5 CLIMOD Simulation Execution Procedures

The general procedure for executing a CLIMOD simulation begins with installing the required files and directory structure and paths. This must be done simultaneously for each platform that is being used. Currently five systems are in use so simulations are done for five separate years. The simulations are initiated and controlled by a main script, once the setup is completed. The only limitation to the number of simulation days that can be executed at one time is the available disk space to store the output data. Once a simulation day is completed the person monitoring the runs is notified

2-6 Quality Control Procedures During CLIMOD Execution

Extensive quality control procedures have been developed using an HTML-based system on an in-house web site (Attachments 7 and 8). This allows continuous monitoring of the individual days both across grid and at point locations. Once a simulation day is completed the person monitoring the runs is notified so they can perform the quality control checks on the output. There are scripts that automate checking for proper file size, missing output, and proper format. The next step is to look at the plotted gridded data for meteorological soundness. Finally, selected individual station point locations of simulated observations are compared with actual observed observations for the same time and point. If the output data is not meteorologically sound investigation then takes place to determine the cause. This occurs quite often when CLIMOD is first applied to a new location, as certain parameter values such as initial soil moisture content may have to be modified. The modifications continue until the model runs consistently, which has taken about a week for the two theaters. Occasionally the run stops because of such things as bad atmospheric data or network problems. A checklist for determining the reason the run stopped and corrective action procedures have been established for each problem. A semi-automated restarting procedure has been established and is continuously being improved.

3.0 - Computational Issues

Several computational issues had to be faced concerning both the platform and the operating system required to meet a climate production capability.

3.1 Computational Platform

Extensive research of the latest workstation technology was conducted to define the optimum workstation and operating system currently available within the cost constraints of the project budget. Based on cost considerations, the decision was to use DEC Alpha "clones". The specific systems used were three 500 MHz Alpha, and two 600 MHz Alpha processor systems. As is typical when using new systems, several hardware and software issues related to system compatibility had to be resolved in order to use the clones effectively, but they were resolved.

3.2. Operating System.

In order to maximize the productivity of the resources available for the project, MESO obtained and installed the Redhat Linux operating system. Redhat Linux is considerably lower in cost for the same expected performance level than a system utilizing operating systems from "brand" name vendors such as Digital UNIX. A Microway Linux Fortran compiler for compiling MASS was also purchased and tested. This compiler is considerably less expensive than the Digital Fortran compiler. Several problems had to be overcome associated with the Linux operating system. Even though MASS was successfully compiled and executed using the Microway compiler under Linux, the performance of MASS never came close to the performance it can achieve when compiled using the DEC Compiler. MESO worked with Microway in an attempt to find the solutions to optimize the performance of MASS (under the Microway compiler) with limited success. The final best solution at this time was found to be compiling under the Digital operating system using a DEC Fortran compiler and then porting the compiled MASS program to the Linux systems.

4.0 -Methods to Composite Climate Data

It was necessary to develop a post-simulation method for blending observations and model generated data. The objective is to develop a method that will yield a single seamless and consistent database in such a way that the simulated statistics surrounding sites where observed data is available closely reflect the observed data. At the same time, the statistics in regions without observed data are specified from the model-simulated data. This may appear to be somewhat redundant since the intention is to assimilate all or most of the available observed data into the model simulations. Thus, the model-generated database will already be a type of blend between the observational data and the model physics. However, the model is capable of simulating only a portion of the variance of each parameter because it cannot simulate atmospheric features that are below the resolvable scale of the model grid. Of course, using a grid mesh finer than 10 km could eliminate this problem. However, that is not computationally feasible. Sub-grid scale parameterization schemes attempt to account for some of these features but they do not model all of the variability found at small scales. This is particularly true for variables such as precipitation, which exhibit a great amount of small-scale variability. Importantly, many extreme events (e.g. isolated heavy rains associated with thunderstorms) are associated with small-scale variability. The purpose of the post-simulation blending technique is to create a single database that will contain most or all the attributes of the observational statistics where they are available and blend smoothly to a model-generated database in other areas.

The formulation of the blending method is based on the principle that the statistical database should be heavily influenced by the observational data near the actual observing sites and blend smoothly into the model statistics away from observational data sites. The final composite climatology should also contain the full distribution of data, not just means and variances, so that a large suite of statistical parameters can be obtained.

The blending procedure uses a weighted average of model and observational data. The weights depend upon the spatial statistics of each variable. In some regions and in some directions the extent of the region of high spatial correlation will be larger. In these cases the impact of the observational data will likewise reach further. The spatial correlation depends on a variety of factors including the terrain, the atmospheric dynamics, and the time of year. An estimate of the spatial correlation is obtained by inter-comparing the large grid simulations, the nested grid simulations and observational data where available.

4.1 Results of Method Investigation

Results from Saint Louis University's (SLU) evaluation determined there are four distinct methods to blend or composite the observed data. All are based fundamentally on some form of distant weighting from the observed site. The difference in the methods is in the way that the autocorrelation function relating the distance and the weight is determined. The four methods are:

(a) Imposed Autocorrelation. The distance autocorrelation is calculated based on derived relationships and reasonable meteorological assumptions associated with such factors as terrain, slope and proximity to water.

(b) Observation Derived Autocorrelation: The autocorrelation function is calculated based upon the relationship found between observed sites. The major disadvantage is the lack of a sufficient density of sites.

(c) Model Derived Autocorrelation: The autocorrelation function is calculated based upon the relationship found between model grid points. The advantage is there is adequate grid coverage. The disadvantage is the method will increase computational requirements.

(d) A Composite Autocorrelation: This would use a blend of the three methods. It is likely that this would produce the best method, but will require more research beyond the scope of this project.

The decision was made to proceed with the imposed autocorrelation method for several reasons. The primary reason it is that any reasonable autocorrelation method is likely to produce acceptable results. Secondly, the method is less computationally intensive than the other methods. Finally, with a "better" method, the expected improvement would be slight and not worth the computational increases. However, this is an area where further improvements could probably be made to the method with additional research.

Analysis of model results indicates that the model statistics differ by only a small amount so that the blending should only make small adjustments. However, quantifying the differences in blending algorithms is an area where further improvements could probably be made to the method with additional research. As part of the current project tasks, the estimated improvement in the climatological statistics that can be obtained through the use of the blending approach will be rigorously tested.

4.2 Description of the Method.

The first step in formulating the blending algorithm is to determine the weights for the model and blended observational data. The blended value is related to the model and observations by:

$$T_i^B = w_{mi} T_i^M + \sum w_{ij} T_j^{Obs} \tag{4.1}$$

Where T_i represents the variable be blended at the grid point i (in this case temperature, but any variable could be substituted), w is the weight given to the model and observations at each respective gridpoint, and the superscripts B,M, and Obs denote the blended, model and observational data respectively. The subscript i refers to the grid point and the subscript j refers

to the station location. The weights for the observational data are obtained by solving the standard system of equations associated with particular algorithm.

The version considered initially was one where the weights were determined by the variation in the terrain from the observing site to the center of the grid point under consideration. In particular, the weights are proportional to:

$$w_{ij} \propto \frac{1}{1+D} \tag{4.2}$$

Where D is the distance from the observation point defined as:

$$D = \int_l (n_{ij} - n(l))^2 dl \tag{4.3}$$

n_{ij} is the normal vector to the surface at the observation site and n(l) is the normal to the surface along the great circle path from the observing site to the model grid point.

The weight for the model value (at the grid point) is determined by the condition:

$$w_{mi} + \sum w_{ij} = 1 \tag{4.4}$$

There are several degrees of freedom in this procedure, which include the overall proportionality constant for w_{ij} and the resolution at which the normal vector integration is determined. Both of these effects act to "control" the reach of the observational data.

The second method used to blend the observations was a hybrid of the above scheme. In this scheme the weights w_{ij} are modified by the weights used in the MASS model initialization scheme to include observations. This optimal interpolation scheme determines weights from the following system of equations:

$$\sum \alpha_{ij} P(r_{ij}) = P(r_{0j}) \tag{4.5}$$

Where $P(r_{ij})$ is the assumed correlation between site i and site j and $P(r_{0j})$ is the correlation between site j and the model grid point. The correlation is distance based and is given by:

$$P(r) = \sigma[(1+\varepsilon)e^{-\lambda(r/R)^2} - \varepsilon]e^{-\lambda(r/R)^2} \tag{4.6}$$

Where r is horizontal distance between the two observations to be correlated, R is the radius of

influence and σ, ε, and λ are adjustable parameters. More details are given in the MASS model reference guide (1994). These weights are then multiplied to the terrain-based weights to obtain the final blending weights.

Both of these blending algorithms were applied to one month of January simulations for upstate New York. The differences in the resulting statistics were quite small and the differences between the blended and original model statistics were also quite small. Most of the changes appeared to be bias corrections in the neighborhood of observational data.

The above blending algorithms do not strictly follow the Optimal Interpolation (OI) procedures. The difference between the two algorithms is in how the model data is incorporated into the blending. Above the model was treated as just another observation, but in OI the model is treated as a first guest (or background estimate). It is possible that an OI scheme will produce better results. The described algorithms are being adapted to follow an OI treatment of the problem for comparison with results obtained from the described method.

5.0 - Determining Simulated Climate Data Quality

The goal of this task is to develop an automated procedure to objectively measure the quality of model-simulated (CLIMOD) climatologies in both data rich and data sparse regions and thus provide an indication of the reliability of the CLIMOD statistics. The CLIMOD technique has the capability to generate climate statistics anywhere in the world. However, the statistics will not be of equal quality due to many factors including the amount and type of input data available for the numerical simulations and the particular model physics and resolution (which may vary due to availability of computational resources) used to generate the climatological dataset.

As SLU has progressed they found that there are two separate subdivisions or subtasks to this effort. The first subtask is the assessment or validation of the climate statistics in the vicinity of observations. At these locations a direct measure of the accuracy of the statistics is available and hence the quality can be determined. The second subtask is an estimate of the confidence of the climate statistics at the locations where observational data are not available. Confidence is NOT a direct measure of accuracy but a indirect measure of the expected quality of the data. So, for the very data sparse region the confidence may be indicated as low only because we have no objective way for determining the quality of the simulated statistics. It is possible that the statistics in a low confidence location are actually very good, there is just know way of objectively determining the representativeness of the statistics

5.1 Assessment of the Method

The assessment procedure is based on the procedure developed in the proof-of-concept phase of this research. The assessment must be done against independent data so the procedure has two steps. The first step is to identify and withhold certain observational data from the simulation procedure and the second is the comparison of these withheld data to the model statistics.

To identify which stations are suitable for the assessment, SLU developed a clustering algorithm that groups stations of similar characteristics. From each of the clusters, one or more stations are chosen to be withheld based on geographical and length/quality of the record. For practical purposes a minimum of 10 and not more than 30 stations should be withheld.

The assessment procedure established in the proof-of-concept was designed to establish the accuracy of the model statistics at the model resolution from station observations. The technique identifies three factors which can be used to define the error in the climate statistics: (1) the bias, (2) the difference in standard deviations between model and observations, and (3) the difference in shapes between the model and observational distributions.

These three can be combined into a single quantity that provides an easy assessment of the climate statistics. While this assessment procedure has been carried out for the upstate New York study, the Korea or Mideast domains have yet to be done. Examples of these quantities are found in the technical reports for the upstate New York January and July simulations.

5.2 Confidence Estimation Method

The estimation of the confidence/quality of the model-generated statistics in data void regions requires alternate approaches based on the dynamics of the region. In these regions, use of satellite data, error models, analogs, and interpolation of known errors are being examined. All of these approaches have weaknesses. Satellite information is often large scale so much of the mesoscale variability is lost. Consequently, satellite data can only be used to provide consistency checks. Error models rely on statistically and empirically determined parameters obtained from the numerical model. Thus, error models provide no external validation of data. Analogs assume that accuracy in one region translates into accuracy in another region with similar characteristics. Interpolation of known errors (from the observational sites) assumes that the error structure function is relatively large scale. The upstate New York results suggest the error structure is mainly large scale but further investigations are planned for the Korean simulations.

Determining the confidence of the climate statistics in data sparse regions may include several of these procedures and possibly others. Consequently, the final confidence product generated should be flexible enough to include a variety of procedures.

6.0 -Analysis of CLIMOD Output

The global grid point analysis data from the NCAR/NCEP Global Data Assimilation System (GDAS) Reanalysis project and all available rawinsonde and surface data were used as prescribed in the procedures outlined in Section 2.1 to create a 3200 km by 3200 km 40 km resolution and a 800 km by 800 km 10 km resolution hourly 3-dimensional dataset for the basic model variables (pressure, temperature, moisture, wind) for a10-year period (1973-82) for the following 2 regions of interest: Korea and the Middle East. The hourly and climate data is being archived for each region on Exabyte high density 8 mm tape. The process of evaluating the output is still in progress at this time. The results of the climate statistics shown here should be considered as early results and not conclusive. The quality of the 10-year datasets are being objectively and subjectively evaluated in each region using all of the available observational data.

6.1: Evaluation of Korean Simulated Climate Data

The results for Korea are represented by Osan Air Base (RKSO) located at 37.08 N and 127.03 E with an elevation of 12 meters.

a. Pressure

The proof-of-concept study conducted on the eastern Great Lakes region showed two problems with the modeled pressures. One problem was an approximately 4 mb bias in the model pressures (both for 10 km and 40 km models). This consistent bias was due to imbalances

introduced by the lateral boundary conditions. Consequently, a mass imbalance was established with more mass leaving the model domain than entered it. This caused the modeled pressure to have a low bias. The lateral boundary condition algorithms were adjusted to ensure the lateral boundary conditions are in mass balance, which helped to eliminate this bias.

The second problem highlighted in the proof-of-concept project was an absence of the diurnal pressure cycle. The reason for this was the fact that the diurnal solar thermal tides have never been built into mesoscale models. A diurnal pressure correction was added as a post processing step to the pressure field. The results to this point indicate that there is considerable improvement in the model pressure. The results in Figure 1 are for Osan Air Base. The figure depicts that the MASS model 10 Km modeled pressure curve clearly captures the diurnal pressure cycle.

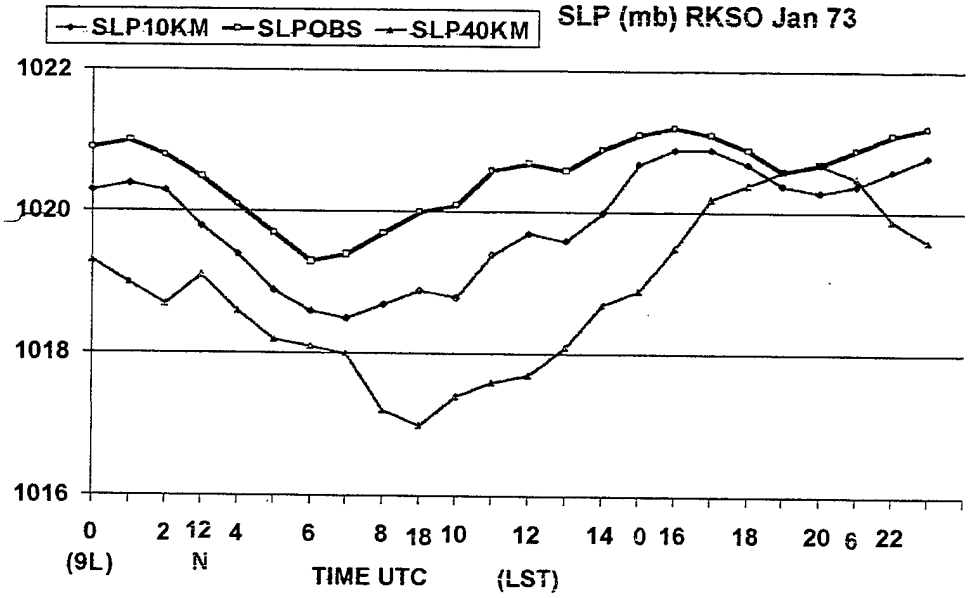

Figure .1. Hourly mean sea level pressure (SLP) comparison for the observed (OBS), 10 Km and 40 Km diurnal pressure curve for the month of January 1973 at Osan Air Base (RKSO).

b. Temperature.

The temperature comparison was consistent with the results from the proof-of-concept research as it again proved to be the best-modeled element. One difference noted was that the 10 Km results were improved over the proof-of-concept results. The reason for this was a change in data assimilation strategy that included using rawinsonde data for the 10 Km as well as 40 Km domains. Also, the PBL scheme was change to TKE for the 10 Km domain. The combination of changes to the PBL scheme and data assimilation resulted in very representative temperature

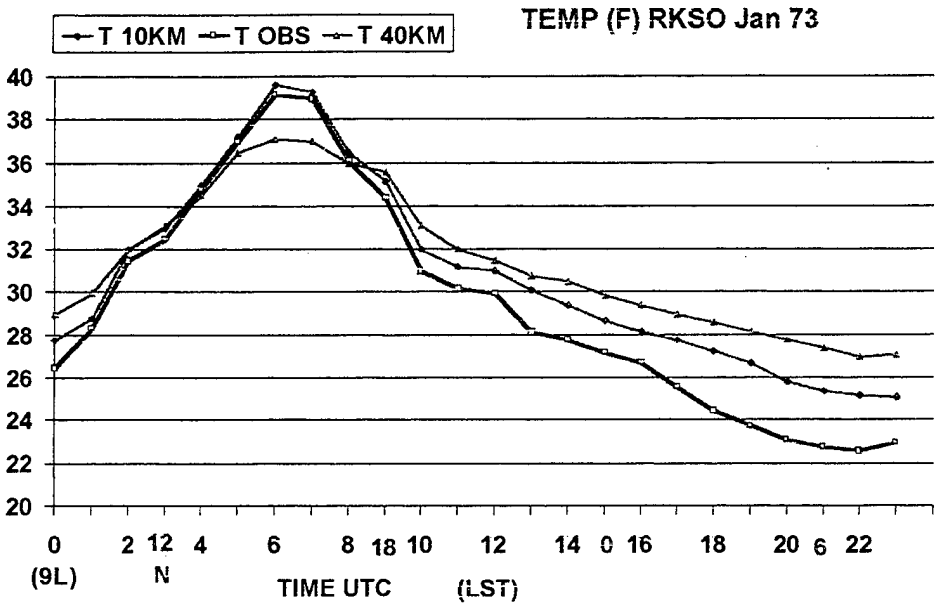

statistics for Osan for both the 10 Km and 40 Km domains as indicated in Figure 2.

Figure .2. Hourly mean surface temperature (T) comparison for the observed (OBS), 10 Km and 40 Km diurnal pressure curve for the month of January 1973.

c. Dewpoint

The modeled dewpoints are also very representative. At 40 Km resolution, a warm dewpoint temperature bias similar to that found in the proof-of-concept was observed. However, the 10 Km dewpoint results were much improved as indicated in Figure .3. The improvement

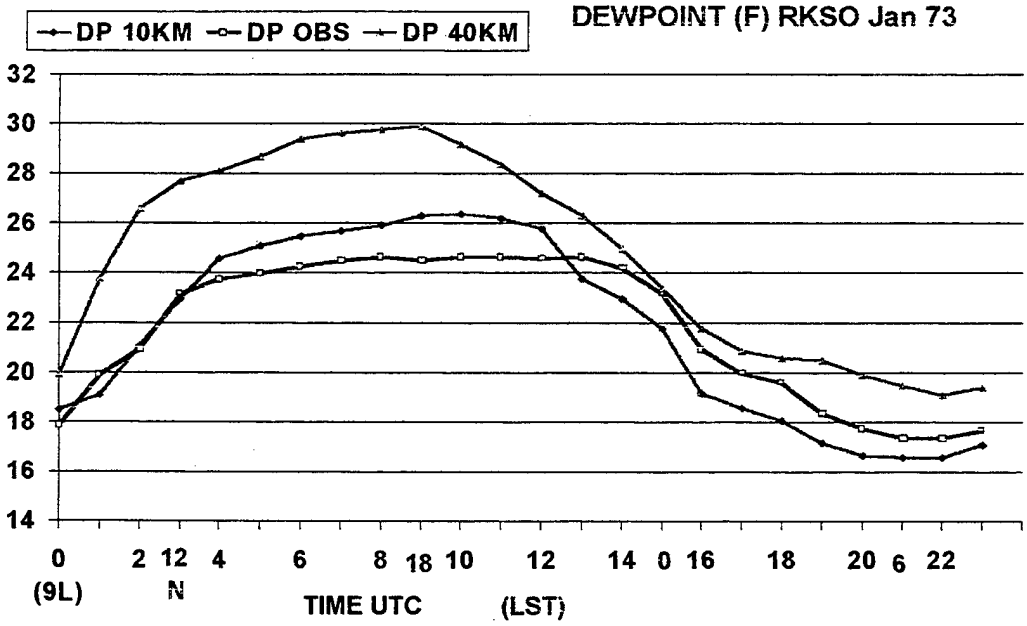

Figure 3. Hourly surface dewpoint (DP) temperature comparison for the observed (OBS), 10 Km and 40 Km diurnal pressure curve for the month of January 1973.

in the 10 Km results is attributed to the change in data assimilation strategy and using the TKE PBL scheme.

d. Wind Speed.

The analysis of the wind speed at Osan in Figure 4 reveals the observed wind speeds were slightly greater during daylight hours than the simulated wind speeds. The 10 Km simulation was somewhat better than the 40 Km domain at capturing the daytime maximum that occurs in the mid afternoon. The nighttime simulated wind speeds were higher than observed. This is likely due to the inability of the model to capture shallow inversions at night resulting in higher modeled wind speeds.

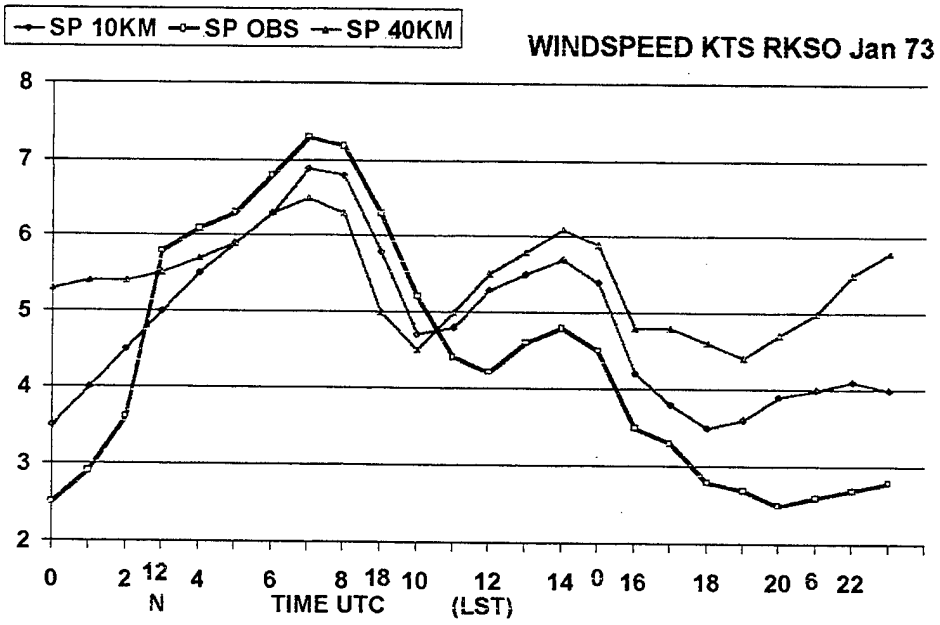

Figure. 4. Hourly mean surface wind speed (SP in knots) comparison for the observed (OBS), 10 Km and 40 Km climate statistics for the month of January 1973 at Osan AB (RKSO).

e. Precipitation

The frequency of precipitation compared reasonably well with the observed at both the 40 Km and the 10 Km resolution (Figure 5). The frequency of precipitation is defined here as the fraction of the days in the month for which rain occurred atthe indicated hour of the day. No clear diurnal pattern was observed in either the observed or the simulated data, and it was not clear that the 10 Km modeled data was more representative than the 40 Km resolution data. However, it is clear the 40 Km resolution simulations produced a smoother (less noisy) curve

than either the 10 Km or observed data. It is likely that all the precipitation curves will smooth as additional years are analyzed.

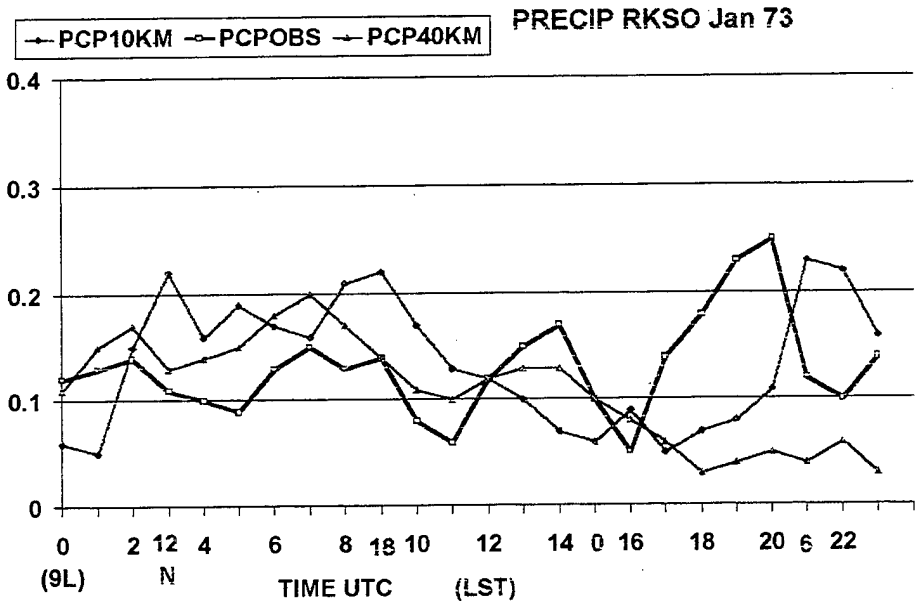

Figure 5. Frequency of precipitation (PCP) occurrence comparison for the observed, 10 Km and 40 Km climate statistics for the month of January 1973 Osan AB (RKSO).

f. Cloud Coverage

Initial steps of establishing methods to model clouds, tops and ceilings, were undertaken. The first step was evaluating the model derived total cloud coverage with the total cloud coverage that is observed. The simulated total cloud coverage is an integrated value for the entire column assuming maximum overlapping of levels. The cloud coverage at each level is obtained by calculating the cloud fraction based upon a simple cloud fraction-relative humidity relationship. The evaluation of cloud coverage is particularly difficult because cloud coverage is not always reported in the observation. However, a limited comparison of the modeled versus observed cloud coverage for Osan AB (Figure 6) revealed encouraging results. Currently, statistics are being generated for ceilings and cloud tops for both Korea and the Mideast. Once compiled, these results will be compared with available cloud observations

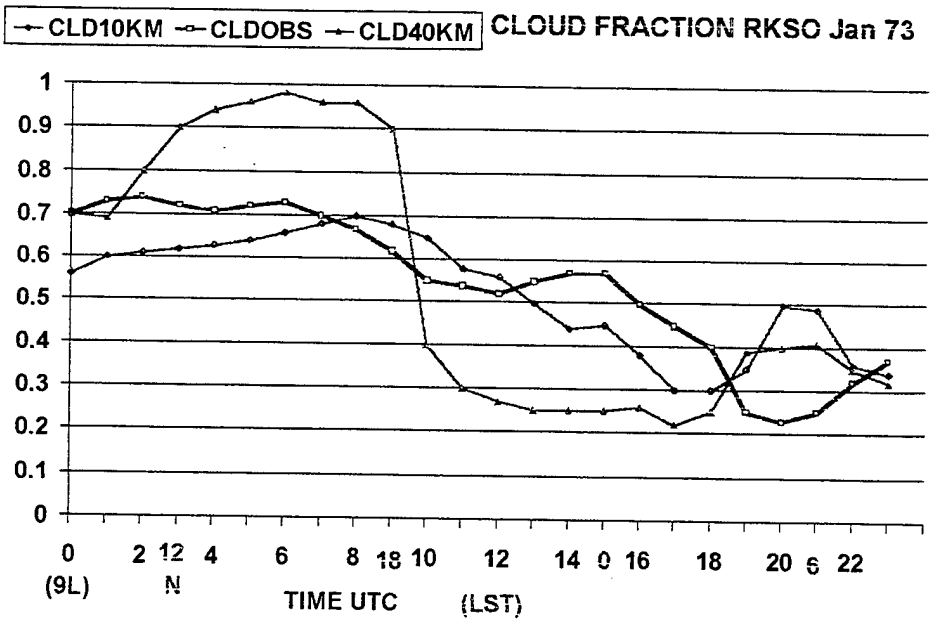

Figure 6. Hourly mean total cloud coverage (CLD) comparison for the observed, 10 Km and 40 Km climate statistics for the month of January 1973 at Osan AB (RKSO).

6.2: Evaluation of Mideast Simulated Climate Data

A limited evaluation of the early results from the Mideast simulation revealed a significant discrepancy in the temperature and dewpoint as the Figures 7 and 8 indicate. The results from 5 January 1973 from Baghdad (32.23 N, 43.15 E, elevation 34 meters) are shown to demonstrate the problems and the results from modifications to the soil moisture to solve the problem. Both Figure 7 and 8 are initial results obtained before soil moisture content was adjusted.

Figure 7 shows a strong overnight warm bias in the modeled temperature. The dewpoint curve at Baghdad for 5 January 1973 depicted in Figure 8 showed an even greater problem with a model warm bias. The possible causes for this were examined. It was determined that the most likely case was an unrealistically high initial soil moisture content. Since the soil in that region is very dry, the model's initial soil moisture content was changed to a near zero value. This greatly improved the results. The Baghdad results depicting surface temperatures and dewpoints for 5 January 1973 using the modified soil moisture content are shown in Figures 9 and 10. The temperature results using the modified soil moisture content decreased the overnight simulated low temperature values. The 10 Km temperature results were improved more than the 40 km results. The modeled dewpoint curve showed a remarkable; improvement when the soil moisture was adjusted as depicted in Figure 10.

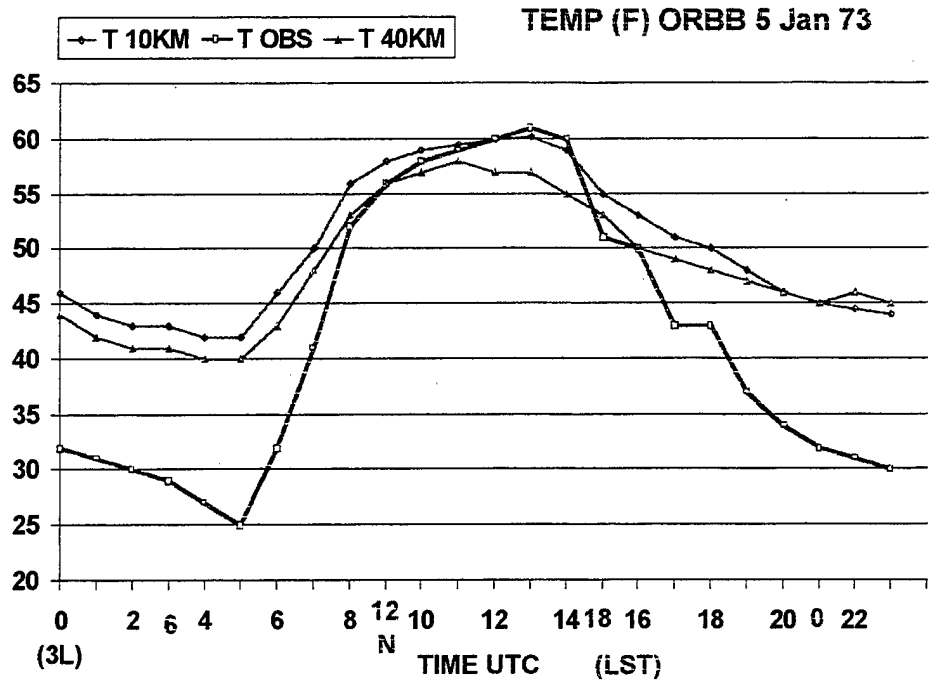

Figure 7. The surface temperature comparison for the observed (OBS), 10 Km and 40 Km domains for 5 January 1973 at Baghdad, Iraq (ORBB) before soil moisture was adjusted.

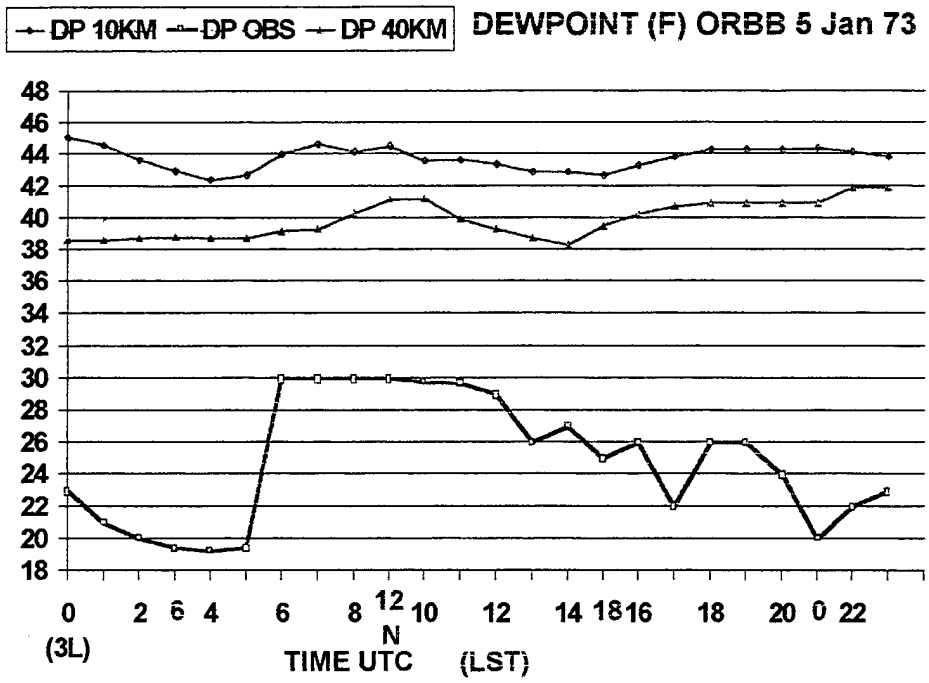

Figure 8. Surface dewpoint temperature comparison for the observed 10 Km and 40 Km for 5 January 1973 at Baghdad, Iraq (ORBB) before soil moisture was adjusted.

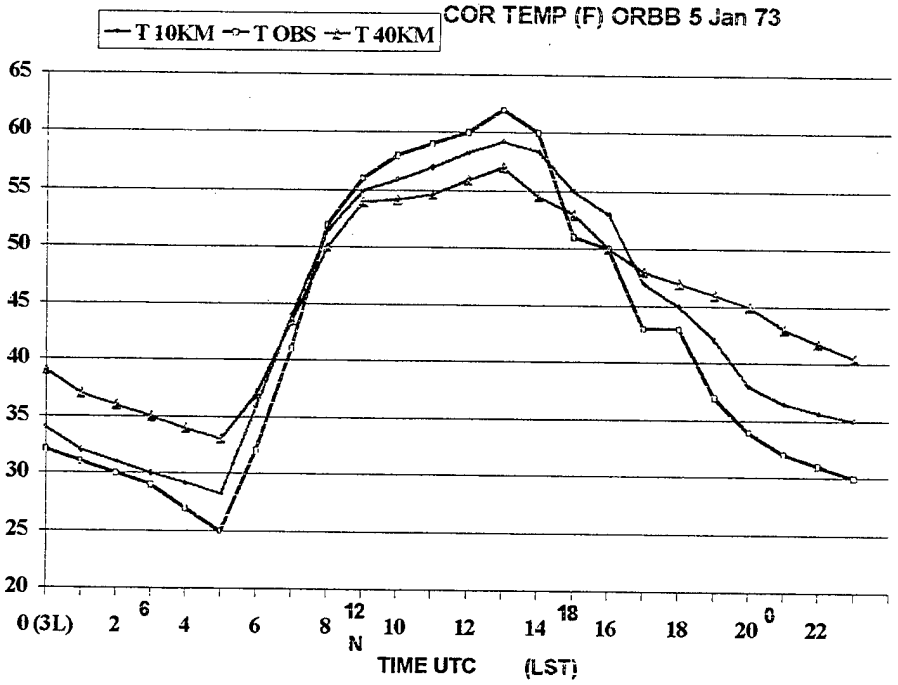

Figure 9. The surface temperature (T) comparison for the observed (OBS) 10 Km and 40 Km for 5 January 1973 at Baghdad, Iraq (ORBB) after soil moisture was adjusted.

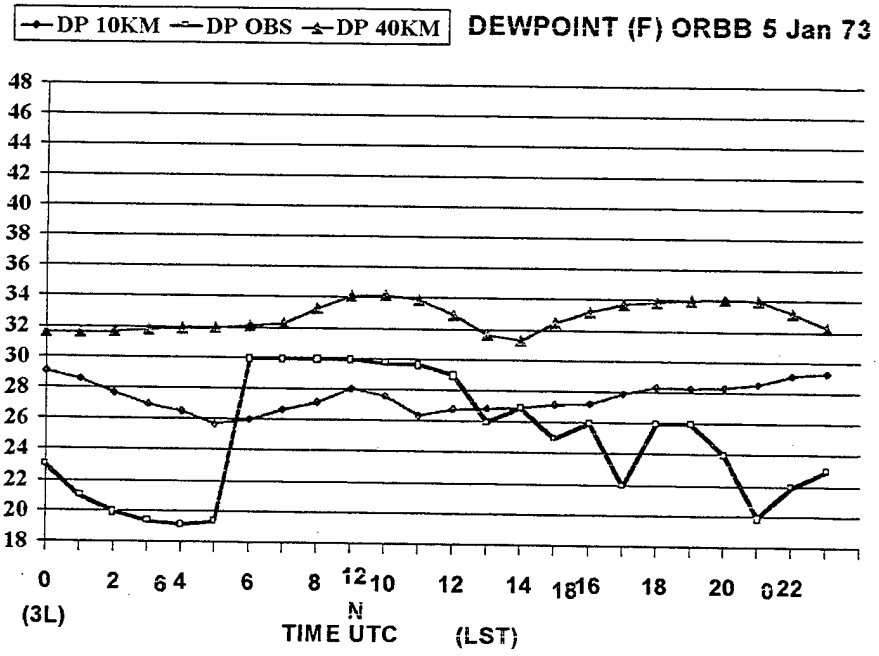

Figure10. The corrected surface dewpoint (DP) comparison for the observed (OBS), 10 km and 40 km for the 5 January 1973 at Baghdad, Iraq (ORBB) after soil moisture was adjusted.

6.3: Construction of the Basic Climate Data Sets

MESO did extensive consultation with AFCCC and its customers to determine the types of basic variable (pressure, temperature, moisture, wind and precipitation) statistics that are desired in the grid point climatologies for each of the two geographical regions. A wide array of products have been produced from four years of the simulated climate data for both Korea and the Mideast in order to examine the quality of the products. Currenttly, MESO, AFCCC and some of its customers, and Saint Louis University are examining the data for quality. Attachment 9 provides an example of a January temperature climatology for the Korean region produced from four years of simulated data. A primary and secondary (i.e. backup) archive of 10-year climatological statistics data and 10 years of hourly simulated data for the coarse and fine mesh grids is being constructed for each of the two regions in Exabyte high-density 8 mm tape.

7.0 - Summary

All indications are that the CLIMOD method will provide high quality climate statistics for both the Korean and Mideast regions. However, the results of the climate statistics shown here should be considered as encouraging early results and not a totally conclusive evaluation. The quality of the 10-year datasets will continue to be objectively and subjectively evaluated in each region using all of the available observational data.

The primary task over the next 12 months will be to finish evaluating the quality of the 10 year datasets. In addition, specific data denial experiments will be performed to help with defining confidence levels and investigation will take place to extend this method to more complex climate variables.

ATTACHMENTS

Attachment 1

Establish Grid Domain

-- 40km/10km Grids

Ingest Atmospheric Data

-- ReAnalysis Grids, Sfc & Upper Air Observational Data

-- Perform 3-D Optimal Interpolation Scheme

Conduct Dynamic Initialization

-- Assure Balance Between Mass & Temperature Fields

Initiate Model Run

-- 12 hour Incremental Analysis Update (IAU) Scheme

-- 6 hourly Boundary Condition Input

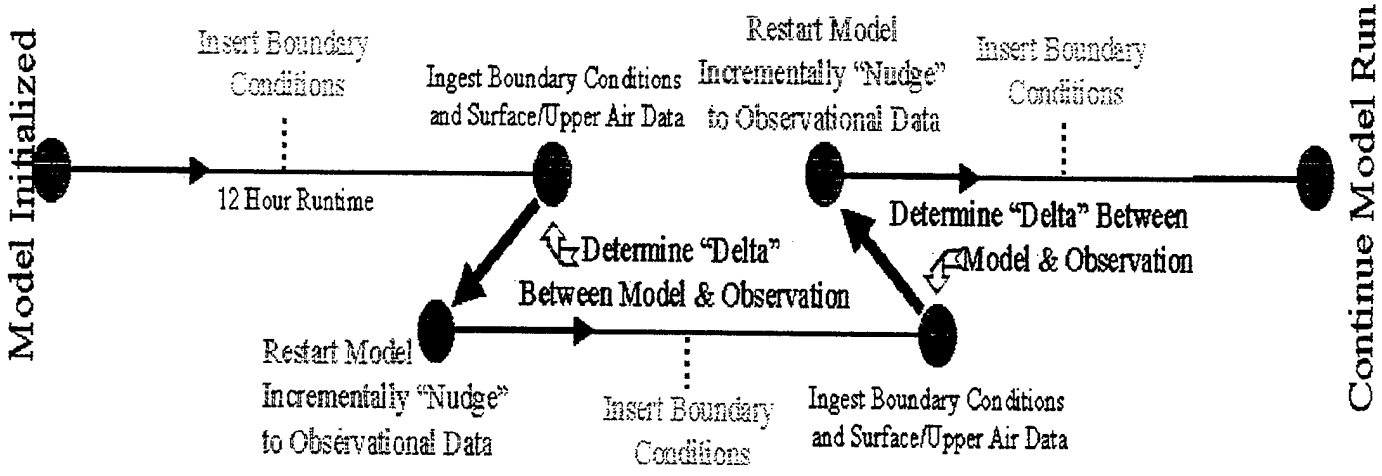

Attachment 2

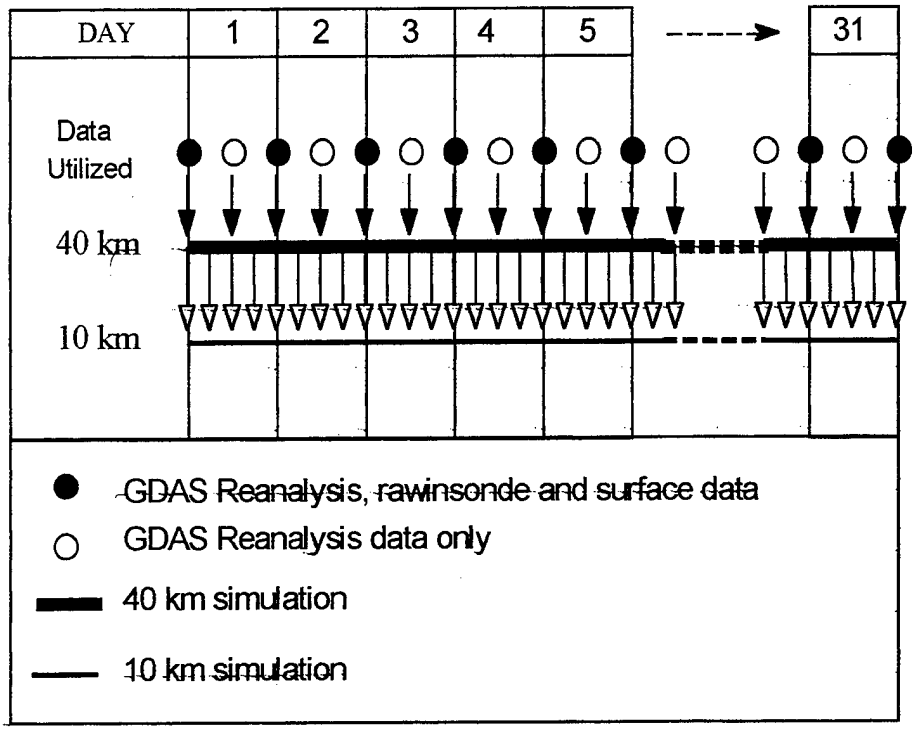

A schematic of the data assimilation strategy used for the generation of climatological datasets during the proof-of-concept research.

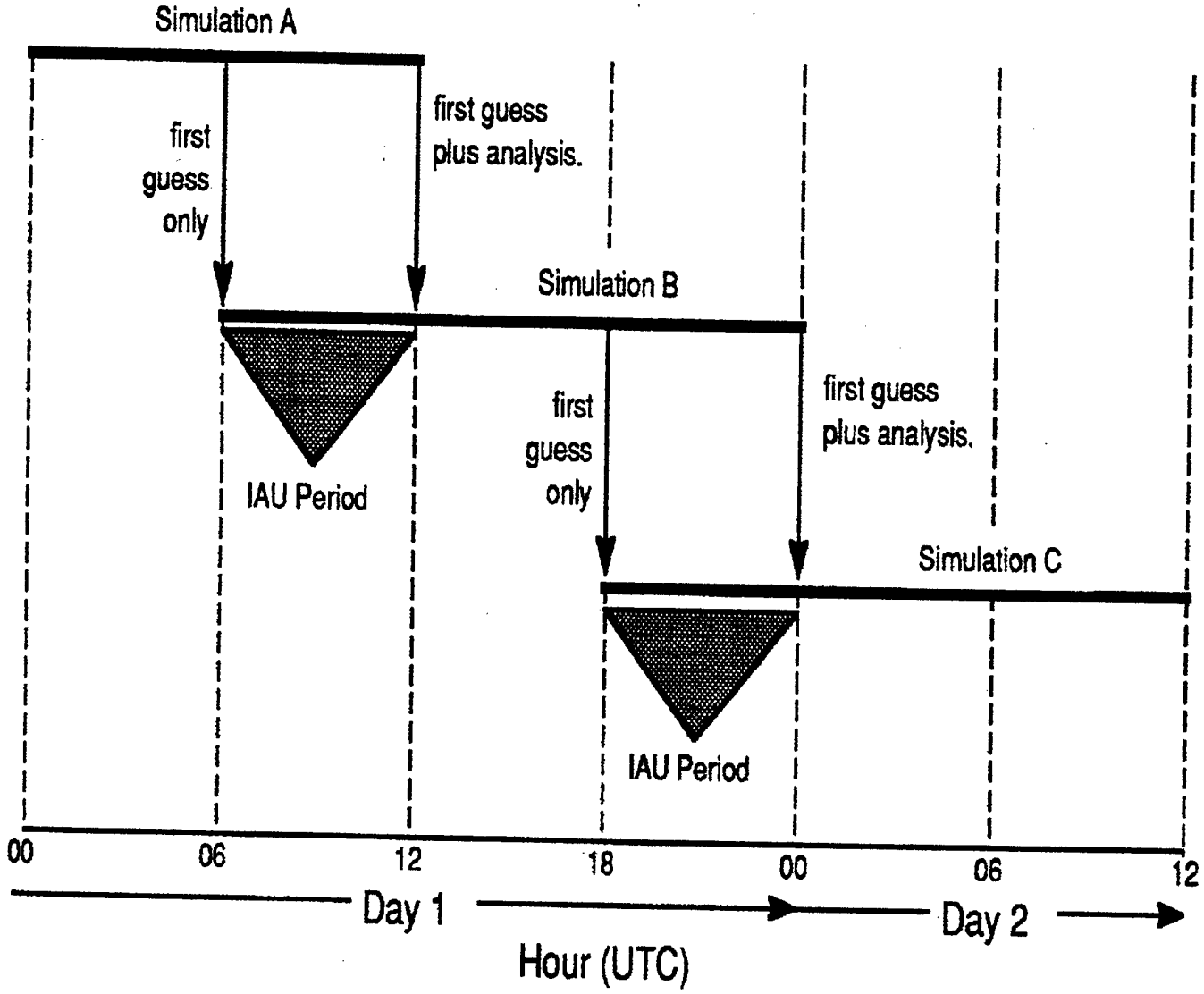

Simulation sequence used in the January 1990 experiment. designed to test the performance of the IAU data assimilation scheme.

Attachment 4

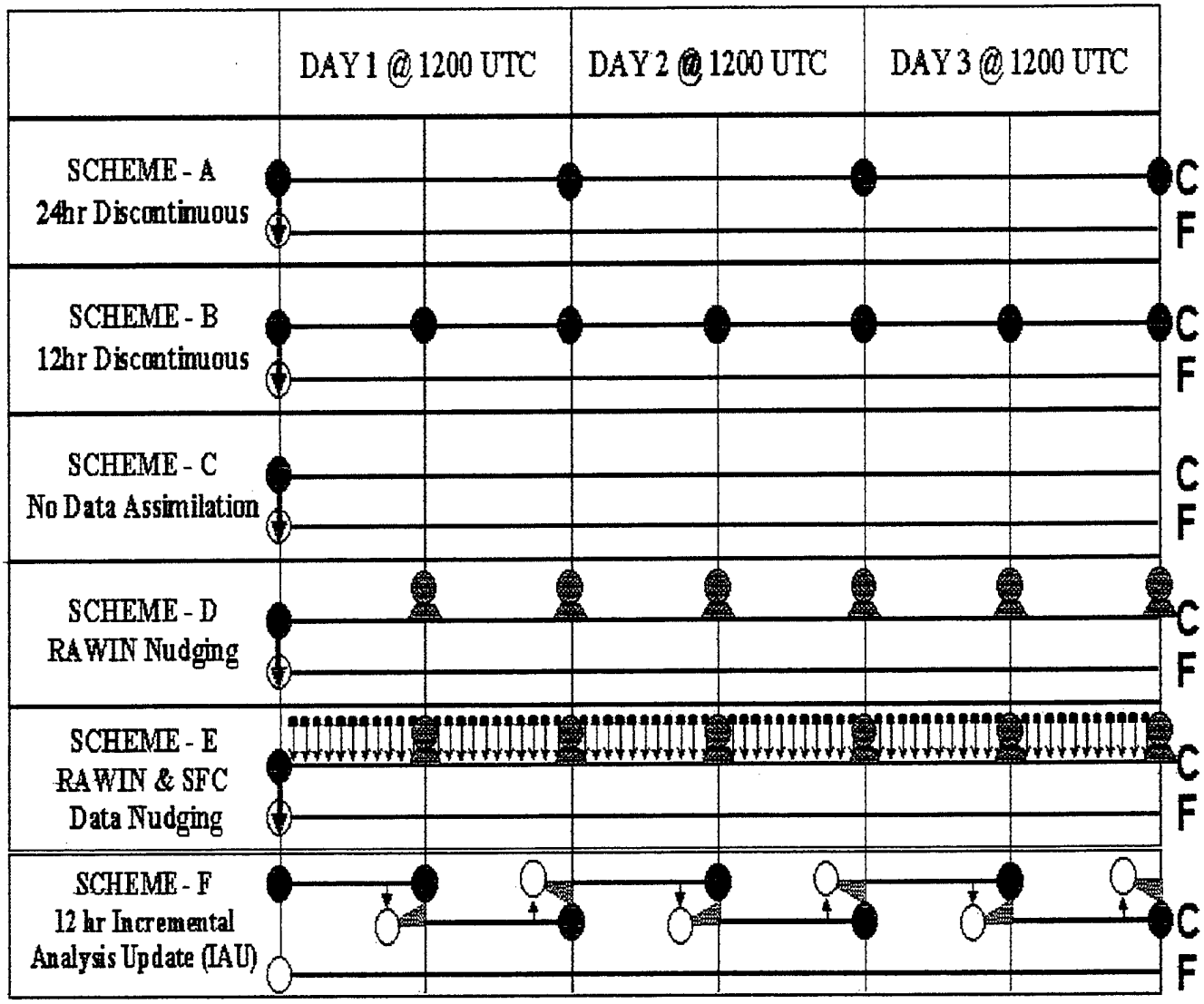

Attachment 5

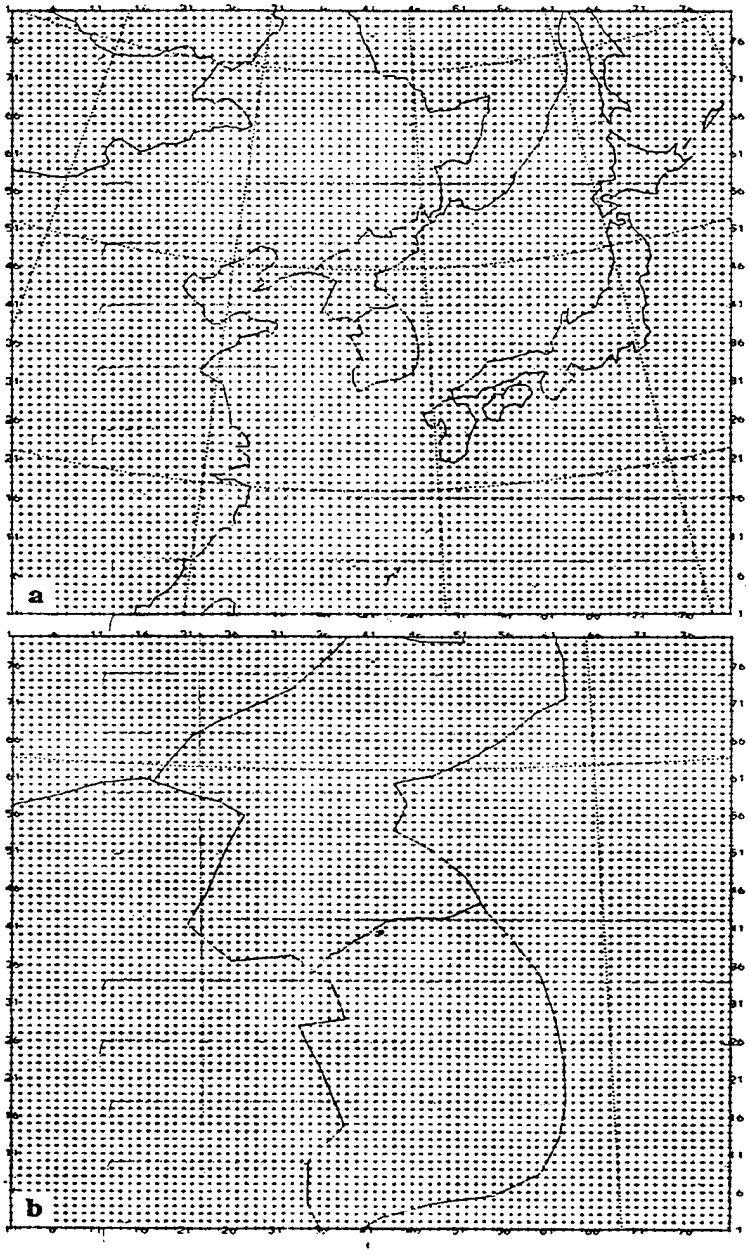

An example of the (a) 40 km and (b) 10 km grid domains that could be employed to generate simulated climate statistics over Korea.

Attachment 6

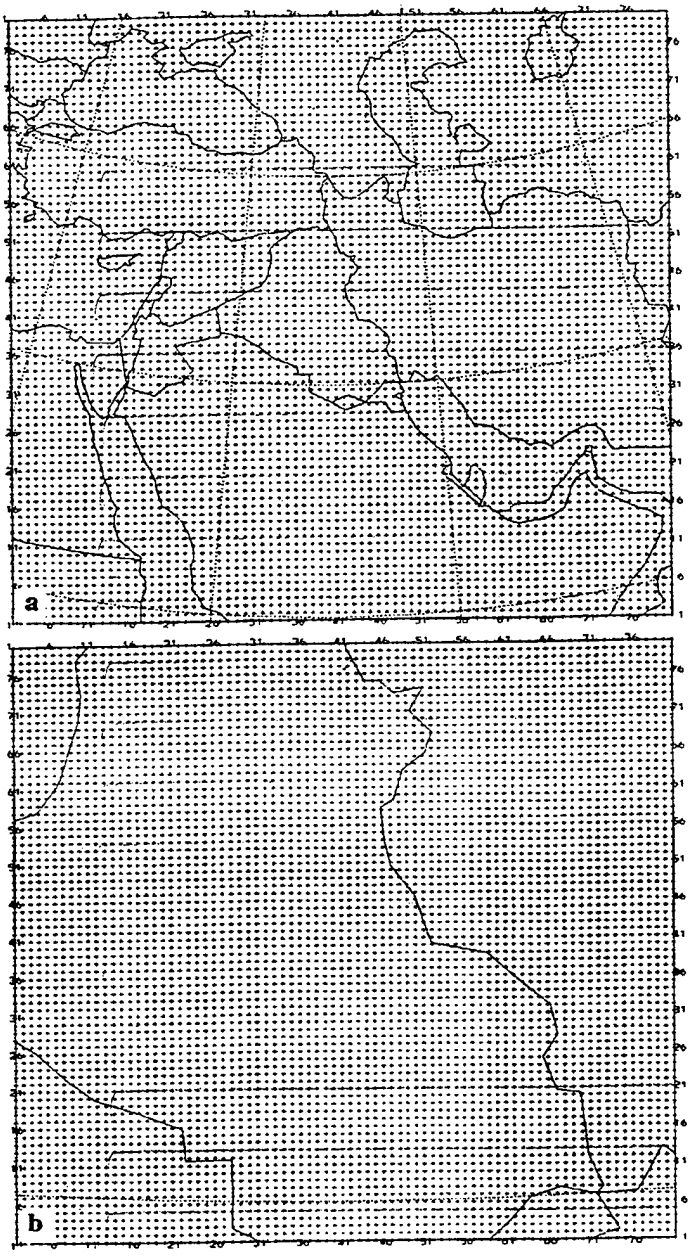

An example of the (a) 40 km and (b) 10 km grid domains that could be employed to generate simulated climate statistics over the Middle East.

HRCP STATUS INFORMATION

Updated at Fri Apr 10 11:42:50 EDT 1998

****

Current Run Information by System

System	Queue Days	First Day	Last Day	Now Executing	Series Start	Est Series End
YANKEE	6	810503	810508	810506	4/ 9/98 2233	4/11/98 117
CARDINAL	6	780407	780413	780410	4/ 9/98 2235	4/11/98 215
INDIAN	5	820511	820515	820514	4/ 9/98 2224	4/10/98 1934
REDSOX	5	730220	730224	ABORTED	4/ 9/98 2223	4/10/98 1755
ORIOLE	6	750219	750224	750222	4/ 9/98 2111	4/10/98 2037

For further information on the runs on each system:
| yankee | cardinal | indian | redsox | oriole

Available System Resource Information

SYSTEM	PARTITION 1 MB	PARTITION 1 DAYS	PARTITION 2 MB	PARTITION 2 DAYS	PARTITION 3 MB	PARTITION 3 DAYS	PARTITION 4 MB	PARTITION 4 DAYS
YANKEE	813.	4.8	1427.	8.4	89.	0.5	495.	2.9
CARDINAL	529.	3.1	1721.	10.1	0.	0.0	0.	0.0
INDIAN	202.	1.2	2061.	12.1	0.	0.0	0.	0.0
REDSOX	1101.	6.5	2264.	13.3	0.	0.0	0.	0.0
ORIOLE	1443.	8.5	1761.	10.4	897.	5.3	3696.	20.0

Archive Status Information by System

SYSTEM NAME	TAPE ARCHIVE LAST CASE	ONLINE DIRECTORY	ONLINE CASE NUM	ONLINE 1st CASE	ONLINE LAST CASE	Questionable Cases in Online Archive Ddirectories < 150 MB in size
YANKEE	K810430	/yank2	5	K810501A	K810505A	NONE
CARDINAL	K780404	/card2	5	K780405A	K780409A	NONE
INDIAN	K820510	/ind2	4	K740630A	K820513A	K820513A
REDSOX	NONE	/red2	6	K790630A	M730221A	NONE
ORIOLE	NONE	/oriole2	6	--------	M750220A	--------

Most Recent Run Information by System

SYSTEM	SIMDAY	BEGDATE	BEGTIME	END DATE	END DATE	40k TIME	10k Time	Tot time
YANKEE	810505	04/10/98	07:20:50	04/10/98	11:37:15	01:23:45	02:38:42	04:16:25
CARDINAL	780409	04/10/98	07:09:17	04/10/98	11:21:07	01:23:00	02:35:27	04:11:50
INDIAN	820513	04/10/98	06:41:43	04/10/98	11:03:12	01:18:50	02:54:50	04:21:20
REDSOX	730221	04/10/98	02:58:20	04/10/98	07:28:04	01:47:19	02:23:46	04:29:44
ORIOLE	750221	04/10/98	04:31:09	04/10/98	08:22:30	01:18:56	02:22:29	03:51:21

High Resolution Climate Project: Korea

Most recently completed run: 40 km

Field	00 hour	06 hour	12 hour	18 hour	24 hour
MSLP/Thickness	0000 UTC	0600 UTC	1200 UTC	1800 UTC	0000 UTC
SFC-500 mb RH	0000 UTC	0600 UTC	1200 UTC	1800 UTC	0000 UTC
850 mb Z/T	0000 UTC	0600 UTC	1200 UTC	1800 UTC	0000 UTC
850 mb Wind	0000 UTC	0600 UTC	1200 UTC	1800 UTC	0000 UTC
500 mb Z/T	0000 UTC	0600 UTC	1200 UTC	1800 UTC	0000 UTC
Surface T	0000 UTC	0600 UTC	1200 UTC	1800 UTC	0000 UTC
Surface Dew Point	0000 UTC	0600 UTC	1200 UTC	1800 UTC	0000 UTC
Surface Winds	0000 UTC	0600 UTC	1200 UTC	1800 UTC	0000 UTC
Cloud Fraction	0000 UTC	0600 UTC	1200 UTC	1800 UTC	0000 UTC
Snow Depth	0000 UTC	0600 UTC	1200 UTC	1800 UTC	0000 UTC
6-hr precip		0600 UTC	1200 UTC	1800 UTC	0000 UTC

Most Recently Completed Run: 10 km

Field	00 hour	06 hour	12 hour	18 hour	24 hour
MSLP/Thickness	0000 UTC	0600 UTC	1200 UTC	1800 UTC	0000 UTC
SFC-500 mb RH	0000 UTC	0600 UTC	1200 UTC	1800 UTC	0000 UTC
850 mb Z/T	0000 UTC	0600 UTC	1200 UTC	1800 UTC	0000 UTC
850 mb Wind	0000 UTC	0600 UTC	1200 UTC	1800 UTC	0000 UTC
500 mb Z/T	0000 UTC	0600 UTC	1200 UTC	1800 UTC	0000 UTC
Surface T	0000 UTC	0600 UTC	1200 UTC	1800 UTC	0000 UTC
Surface Dew Point	0000 UTC	0600 UTC	1200 UTC	1800 UTC	0000 UTC
Surface Winds	0000 UTC	0600 UTC	1200 UTC	1800 UTC	0000 UTC
Cloud Fraction	0000 UTC	0600 UTC	1200 UTC	1800 UTC	0000 UTC
Snow Depth	0000 UTC	0600 UTC	1200 UTC	1800 UTC	0000 UTC
6-hr precip		0600 UTC	1200 UTC	1800 UTC	0000 UTC

MASS Surface Characteristic Fields

40 Km Terrain
40 km Land / Water
40 km Landuse
40 km Vegetation Index (Climatological)

MESO Atmospheric Models | Real-time MASS forecasts | High Resolution Climate Project | MASS documentation | Real-time OMEGA forecasts | MESO

Attachment 9

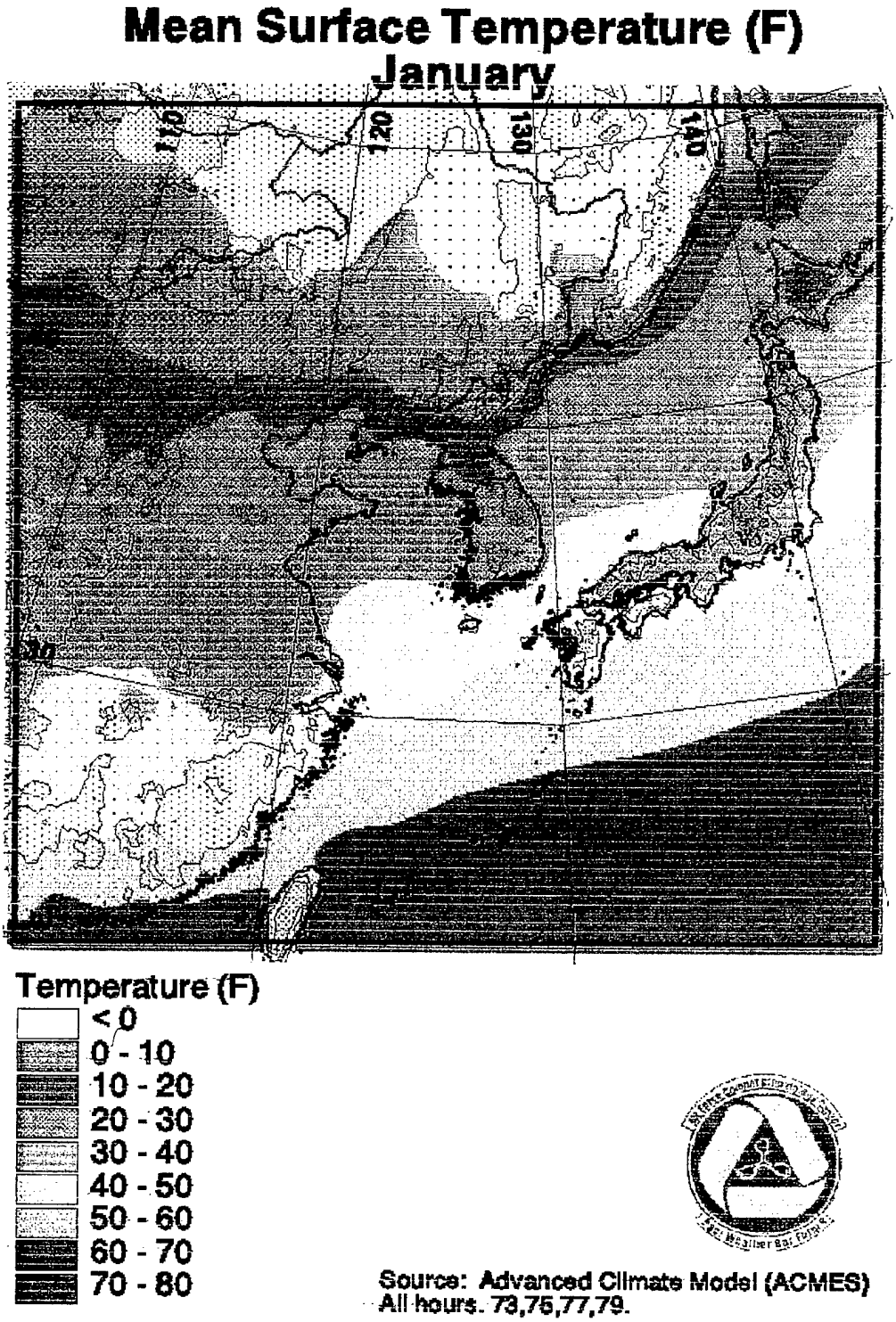

An example of the simulated climatological gridded data produced by CLIMOD.

REFERENCES

Anderson, J. R., E. E. Hardy, J. T. Roach, and R. E. Witmer, 1976: A land use and land cover classification system for use with remote sensor data. *U.S. Geological Survey Professional Paper 964.* U.S. Government Printing Office, Washington, 28 pp.

Anthes, R. A., 1977: A cumulus parameterization scheme using a one-dimensional cloud model. *Mon. Wea. Rev.*, **105**, 270-286.

Blackadar, A. K., 1976: Modeling the nocturnal boundary layer. Preprint, Third Symposium on AtmosphericTurbulence, Diffusion and Air Quality, Raleigh, NC, Amer. Meteor. Soc., 46-49.

_____, 1979: High-Resolution models of the planetary boundary layer. *Advances in Environmental Science and Engineering, Vol. 1*, J. R. Pfaffin and E.N. Ziegler, Ed., Gordon and Breach, 276 pp.

Giorgi, F. and M.R. Rosaria Marinucci, 1996: An investigation of the sensitivity of simulated precipitation to model resolution and its implication for climate studies. *Mon. Wea. Rev.*, **124**, 148-166.

Giorgi, F., G.T. Bates, and S.J. Nieman, 1993: The multiyear surface climatology of a regional atmospheric model over the Western United States, *J. Climate*, **6**, 75-95.

Kalnay, E., M.Kanamitsu, R. Kistler, W. Collins, D. Deaven, L. Gandin, M. Iredell, S Saha, G. White, J. Woollen, Y.Zhu, M.Chelliah, W. Ebisuzaki, W. Higgins, J.Janowiak, K.G. Mo, C. Ropelewski, J. Wang, A.Leetmaa, R. Reynolds, R. Jenne, D. Joseph, 1996: The NCEP/NCAR 40-year reanalysis project. *Bull. Amer. Meteor. Soc.*, **77**, 437-471.

Kaplan, M.L., J.W. Zack, V.C. Wong, and J.J. Tuccillo, 1982: Initial results from a mesoscale atmospheric simulation system and comparison with the AVE-SESAME-I dataset. *Mon. Wea. Rev.*, **110**, 1564-1590.

Kuo, H. L., 1965: On the formation and intensification of tropical cyclones through latent heat release by cumulus convection. *J. Atmos. Sci.*, **22**, 40-63.

Mahrt, L. and H. Pan, 1984: A two-layer model of soil hydrology. *Boundary-Layer Meteorol.*, **29**, 1-20.

Mailhoit, J. and R. Benoit, 1982: Inclusion of a TKE boundary layer parameterization in the Canadian regional finite element model. *Mon. Wea Rev.*, **117**, 1726-1750.

Manobianco, J, J.W. Zack, G.E. Taylor, 1996: Workstation-based real-time mesoscale modeling designed for weather support to operations at the Kennedy Space Center and Cape Canaveral Air Station. *Bull. Amer. Meteor. Soc.*, **77**, 653-672.

Meisinger, and A. Arakawa, 1976: Numerical methods used in atmospheric models. Vol I, GARP Publication Series 17, WMO, Geneva.

MESO, 1994: *MASS Version 5.6 Reference Manual.* MESO, Inc., 185 Jordan Rd. Troy, NY 12180, 118 pp.

Noilhan, J. and S. Planton, 1989: A simple parameterization of land surface processes for meteorological models. *Mon. Wea. Rev.*, **117**, 536-549

Pielke, R. A., 1984: *Mesoscale Meteorlogical Modeling*, Academic Press, New York, 612 pp.

Sasamori, T., 1972: Radiative cooling calculation for application to general circulation experiments. *J Appl. Meteor.*, **7**, 721-729.

REFERENCES

Anderson, J. R., E. E. Hardy, J. T. Roach, and R. E. Witmer, 1976: A land use and land cover classification system for use with remote sensor data. *U.S. Geological Survey Professional Paper 964.* U.S. Government Printing Office, Washington, 28 pp.

Anthes, R. A., 1977: A cumulus parameterization scheme using a one-dimensional cloud model. *Mon. Wea. Rev.*, **105**, 270-286.

Blackadar, A. K., 1976: Modeling the nocturnal boundary layer. Preprint, Third Symposium on AtmosphericTurbulence, Diffusion and Air Quality, Raleigh, NC, Amer. Meteor. Soc., 46-49.

_____, 1979: High-Resolution models of the planetary boundary layer. *Advances in Environmental Science and Engineering, Vol. 1*, J. R. Pfaffin and E.N. Ziegler, Ed., Gordon and Breach, 276 pp.

Giorgi, F. and M.R. Rosaria Marinucci, 1996: An investigation of the sensitivity of simulated precipitation to model resolution and its implication for climate studies. *Mon. Wea. Rev.*, **124**, 148-166.

Giorgi, F., G.T. Bates, and S.J. Nieman, 1993: The multiyear surface climatology of a regional atmospheric model over the Western United States, *J. Climate*, **6**, 75-95.

Kalnay, E., M.Kanamitsu, R. Kistler, W. Collins, D. Deaven, L. Gandin, M. Iredell, S Saha, G. White, J. Woollen, Y.Zhu, M.Chelliah, W. Ebisuzaki, W. Higgins, J.Janowiak, K.G. Mo, C. Ropelewski, J. Wang, A.Leetmaa, R. Reynolds, R. Jenne, D. Joseph, 1996: The NCEP/NCAR 40-year reanalysis project. *Bull. Amer. Meteor. Soc.*, 77, 437-471.

Kaplan, M.L., J.W. Zack, V.C. Wong, and J.J. Tuccillo, 1982: Initial results from a mesoscale atmospheric simulation system and comparison with the AVE-SESAME-I dataset. *Mon. Wea. Rev.*, **110**, 1564-1590.

Kuo, H. L., 1965: On the formation and intensification of tropical cyclones through latent heat release by cumulus convection. *J. Atmos. Sci.*, **22**, 40-63.

Mahrt, L. and H. Pan, 1984: A two-layer model of soil hydrology. *Boundary-Layer Meteorol.*, **29**, 1-20.

Mailhot, J., and R. Benoit, 1982: A finite-element model of the atmospheric boundary layer suitablefor use with numerical weather prediction models. J. Atmos. Sci., 39, 2249-2266.

Manobianco, J, J.W. Zack, G.E. Taylor, 1996: Workstation-based real-time mesoscale modeling designed for weather support to operations at the Kennedy Space Center and Cape Canaveral Air Station. *Bull. Amer. Meteor. Soc.*, 77, 653-672.

Meisinger, and A. Arakawa, 1976: Numerical methods used in atmospheric models. Vol I, GARP Publication Series 17, WMO, Geneva.

MESO, 1994: *MASS Version 5.6 Reference Manual.* MESO, Inc., 185 Jordan Rd. Troy, NY 12180, 118 pp.

Noilhan, J. and S. Planton, 1989: A simple parameterization of land surface processes for meteorological models. *Mon. Wea. Rev.*, **117**, 536-549.

Pielke, R. A., 1984: *Mesoscale Meteorlogical Modeling*, Academic Press, New York, 612 pp.

Sasamori, T., 1972: Radiative cooling calculation for application to general circulation experiments. *J Appl. Meteor.*, 7, 721-729.